

Armando Chavez

Engineering Portfolio



ASU - Capstone Project

Mechanical Engineering Capstone Project: "The Burro" Deployable Car Cover

The capstone project serves as a method of evaluating the mechanical engineering program at Arizona State University through the use of ABET criterion.

Our team worked on creating a sun shade for compact cars that can mount to the trunk and also be stored in the trunk with ease. This design covers the vehicle to prevent damage and resist radiation and conduction heat transfer in a convenient form factor that requires minimal user effort. My role on the team was to design and manufacture each component for prototype using fundamental engineering principles for heat transfer and stress analysis on components/assembly. I drafted detailed drawings of the components from the main rotating mechanism that were sent to the universities machine shop to be manufactured

2.1 Design description Overview

Our prototype design meets the problem statement we had where we wanted a product that can cover a car and deploy over the car within a certain amount of time. We meet the first requirement of covering the car by having more than 20 ft. of rolled fabric within the housing which can be rolled out on top of the car. We believe this was the most optimum design because with a spring loaded mechanism it can keep tension on the tarp when fully extended and it allows the tarp to be retracted and stored easily and effortlessly. Since we didn't want our user to have to fold and unfold a large tarp over their car we needed a mechanism which can store the fabric for us easily which is our spring mechanism as mentioned above. This design helps to reduce the amount of time a person would spend trying to cover their whole car manually with an ordinary car cover.

Figure 2.1.1 Isometric view, side view, zoomed view of mechanism

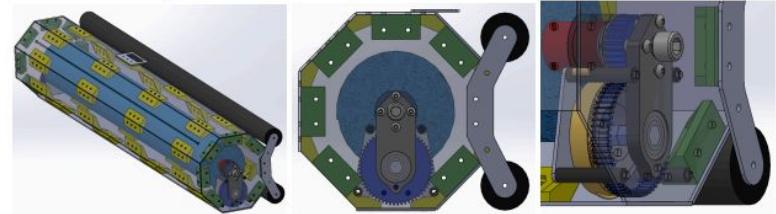


Table 2.1.2 Key Performance Characteristics

Characteristic	Result
Weight	25 lbs.
Dimension	4ft. x 1ft. x 1ft. Exterior dimensions
Deploy time	< 45 seconds

ASU - Capstone Project (Additional)

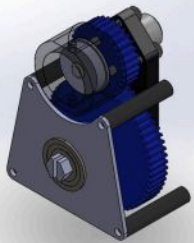


Figure 8.3.1: Internals View 1

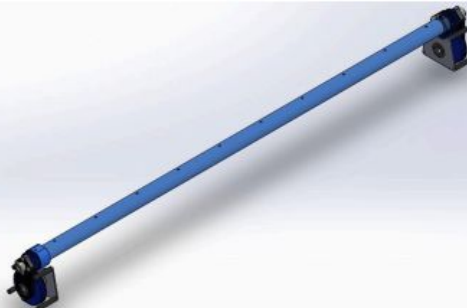


Figure 8.3.3 Complete Internals

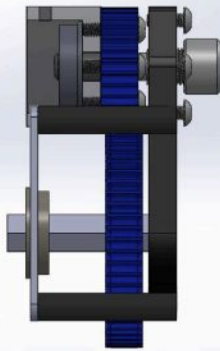


Figure 8.3.2 Internals View 2

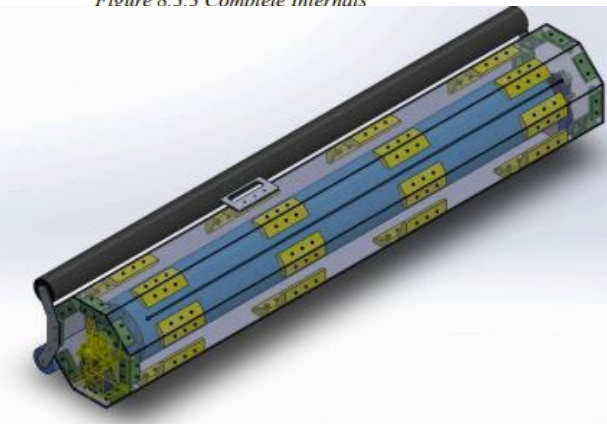


Figure 8.3.4 Completed Assembly

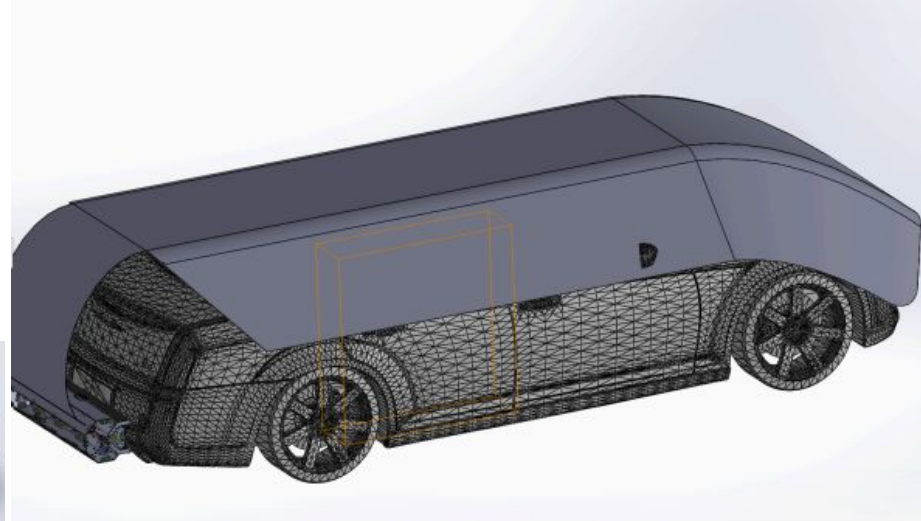


Figure 7.0.1: Updated Cover Deployed

Combustion - Biomass Pellet Burner

Overview/Problem Statement -

Biomass pellet burners are one of the cheapest alternative fuel energy systems that can potentially have a wide variety of applications. They can be specifically useful for the farming industry where large amounts of biomass are produced, commercial and residential sectors as a replacement to traditional fossil fuel burners. Currently, 3kW burner is available to meet smaller energy demands but a strong need for a 40kW burner is expressed by a large market share and our project seeks to address this. Also, currently available pellet burners are exclusive to the European market and are not readily available in the United States. Emissions are a major factor plaguing most burners with stricter emission norms being implemented year after year. The choice of fuel plays a major role in the performance as well as in the emissions from the pellet burner. Overall, the task before us is to design a pellet burner that is cost-effective, limits emission without compromising efficiency and is compact and portable.

Project attached to end of slides...

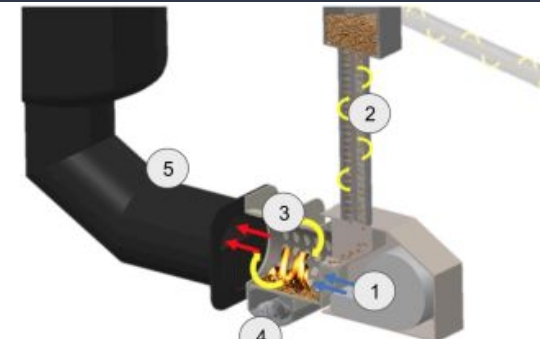


Fig 2: Design Schematic

Label	Description
1	Air blower
2	Pellet Feeder
3	Rotating Combustion Chamber
4	Ash Collector
5	Heat Exchanger

ASU - Structural Analysis Final Project

Overview -

Project description:

A notched rectangular cross-section cantilever beam is loaded in bending. We needed to determine a reasonable finite element mesh and compare its prediction of maximum stress and deflection with a closed form solution for the points at the beam end, location D(given distance along the beam length) and at the location of the notch. For this project 4 different level of mesh were to be considered. Maximum deflection and stress values at point D and at the notch for each mesh condition were to be compared with the analytical values.

Given information/requirements/assumptions:

The beam dimensions/geometry and force/location applied are given along with the material properties. Stress concentration factor K_t at the notch is given. The supporting wall is considered to be much stiffer than the beam and the beam weight is negligible compared to the applied load.

Detailed work at end of slides...

ASU - Shaft Design Project

Overview -

GearBox Shaft Design:

For this project we needed to design 2 gear shafts for a gearbox in an engine/compressor assembly. Our main focus was to determine reasonable shaft diameters for input and output shafts based on the following 4 failure criteria Goodman, Gerber, ASME Elliptic, and Soderberg.

Given information/requirements:

The torque-time function on the output shaft gives us the min and max torque values. The required gear ratio of 3:1 reduces the velocity from input to output and the gear diameters(with a 20 degree pressure angle) were specified to determine forces on each shaft. Stress concentration factors for both bending and torsion were given at the critical location where both moment and torque are largest. Material properties and assumptions about the material like surface finish are given.

Detailed work at end of slides...

GoX Labs Mechanical Engineering Internship - Tempe, Az

GoX Labs -

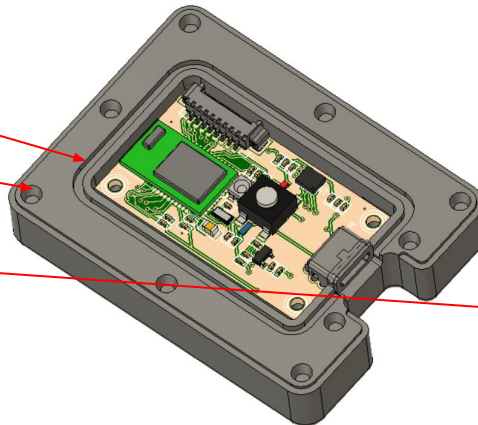
At GoX we strived to understand and improve the health and body mechanics for labor intensive work environments. Using custom designed PCBs and software to measure the body movements of workers in construction sites, our team was able to generate motion patterns and determine how impactful it can be on the human body over time.

My Role at GoX Labs -

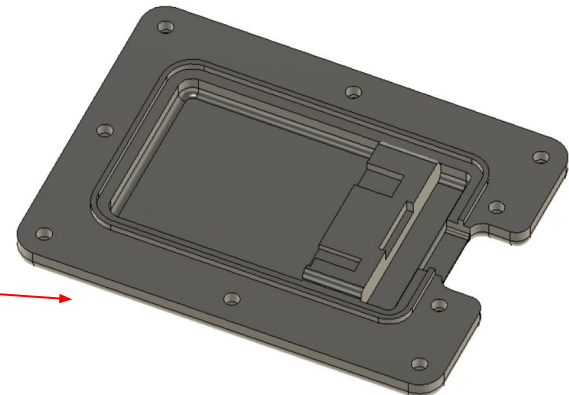
Starting off at GoX I conducted research for off the shelf components to start creating initial case designs for our PCBs. I started designing wearable cases to help our programming team collect motion data. This was accomplished using fusion 360 for the design and in house 3D printers for manufacturing. After various iterations and design meetings we moved to our final stage of production which consisted of silicone injection molding. Using injection molding as our manufacturing process gave us advantages in material properties such as yield strength, which was not attainable with our 3D printed materials. Initially GoX did not have any silicone injection molding setup or procedures, so I was given the task to research and develop our manufacturing process

GoX Labs - NeckPod

- IP67- Water resistant seal
- M2 threaded insert hole locations
- Removable top for access to programming PCB
- Designed NeckPod case using company required software AutoDesk Fusion 360
- Collaborated with electrical engineering team to incorporate mounting and charging locations for PCB



Bottom Half of NeckPod Case



Top half of NeckPod Case



GoX Labs - Insole Pod

- External Button to switch between modes
- Charging port specific for previously purchased cables
- Through holes designed to hide bolt hardware/threaded inserts on top lid
- Integrated loops to secure insole pod to construction boots
- On/Off switch connected to underside of PCB
- Designed to fit curvature of standard construction boot



Carl Hayden Falcon Robotics - Phoenix, AZ

Carl Hayden High School Falcon Robotics -

Our robotics team was heavily engaged in multiple robotic competitions and activities ranging from land, underwater and sky. We competed in FRC FIRST robotics competitions in AZ for regionals and St. Louis for FIRST Championships. During the summers our team also competed in RoboSub, which is an underwater fully autonomous robotic competition at the collegiate level.

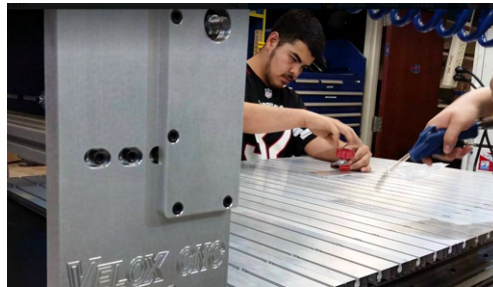
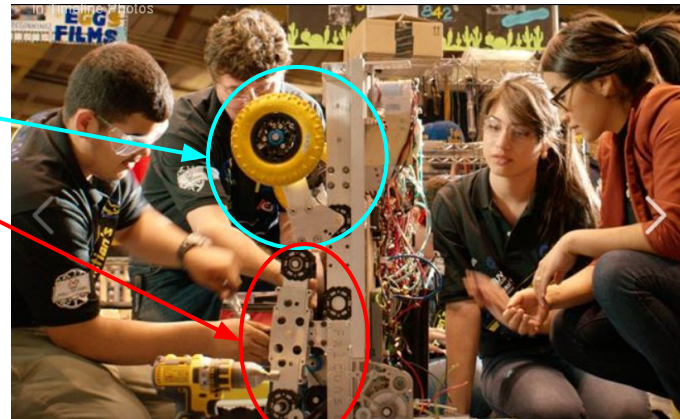
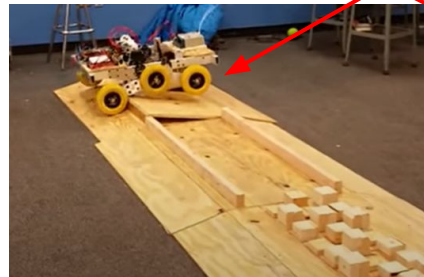
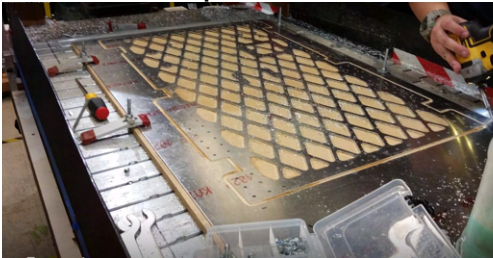
My Role on Falcon Robotics -

I was the mechanical and design lead during my Jr/Sr year. I was in charge of all manufacturing and training members on all machines in our workshop such as the lathe, CNC mill, CNC router, vertical mill, 3D printers, bandsaw, etc. All designs were created using solidworks and CNC toolpaths were created using MasterCam. After raising enough money to purchase our CNC machines, I took initiative to figure out how to operate and program the machines since we did not have any mentors who were experienced in CNC machining.

Carl Hayden Falcon Robotics -

FIRST Robotics Competition (FRC)-

- Nasa inspired rover suspension drivetrain
- Front wheels independently damped via gas struts
- Rear wheels connected to rocker arm assembly via shared pivot



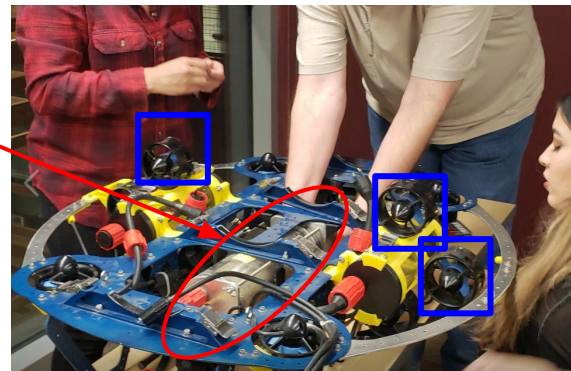
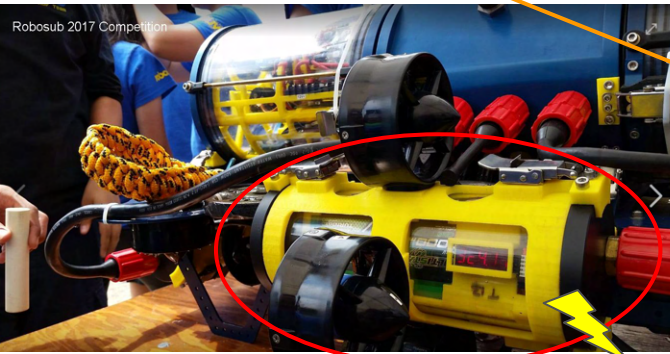
VELOX CNC router -

- 48in. x 48in. X 10in. work area for cutting aluminum sheets/tubes/angle
- Setting up the CNC router to create a subframe for mounting our electronics, pneumatics, batteries, sensors etc.

Carl Hayden Falcon Robotics -

Underwater RoboSub Competition -

- Battery Pods Assembly ⚡
- DVL(Doppler Velocity Logger) assem.
- **Blue ROV thrusters**
- Aluminum waterjet frame with anodized coating for corrosion resistance
- Subconn connectors



Carl Hayden Falcon Robotics -

Underwater RoboSub Competition - Battery Pods

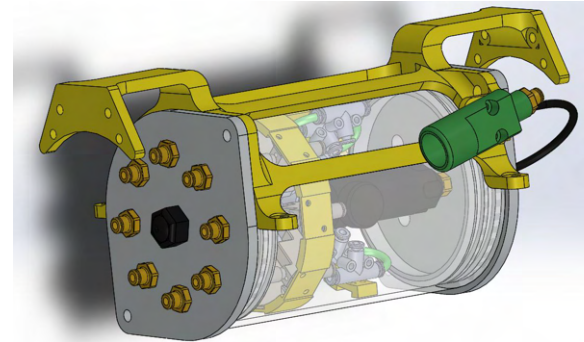
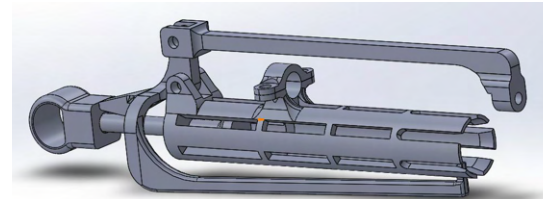
- External battery pods from the main housing to prevent expansion from LiPo cells in case of water damage
- Quick spring latches to easily access batteries for charging after tests.competition runs
- Pressure relief valves on each battery pod to decrease the risk of pressure build up.
- External 3D printed housing to mount BlueROV thrusters and act as mounting supports for the battery pod itself
- Machined end caps from ABS to hold o-rings for a water tight seal



Carl Hayden Falcon Robotics -

Underwater RoboSub Competition - Pneumatic Assembly

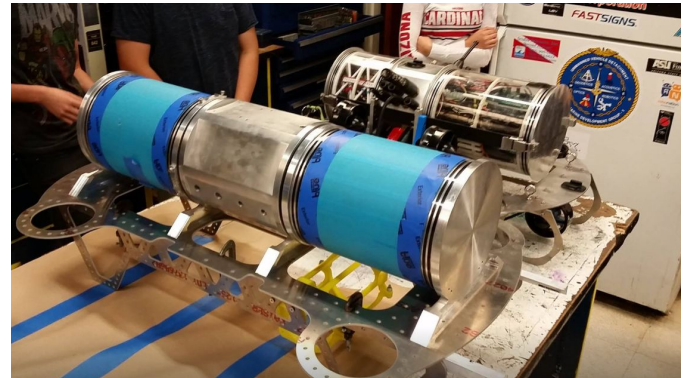
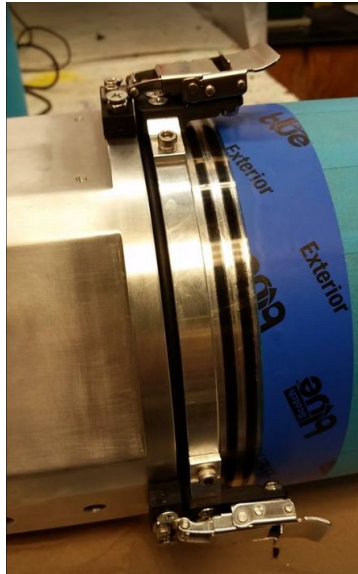
- O-rings/grooves ensure this assembly is water tight.
- There are 8 external auxiliary ports for future expansion when designing external mechanisms such as our torpedo launcher.
- Pressure relief valve to release pressure in case of pressure build up within the assembly
- CO₂ cartridge puncture/adapter
- Pressure regulator, reduces CO₂ pressure from 700 psi to ~ 90 psi (psi limit for our pneumatic cylinders)



Carl Hayden Falcon Robotics -

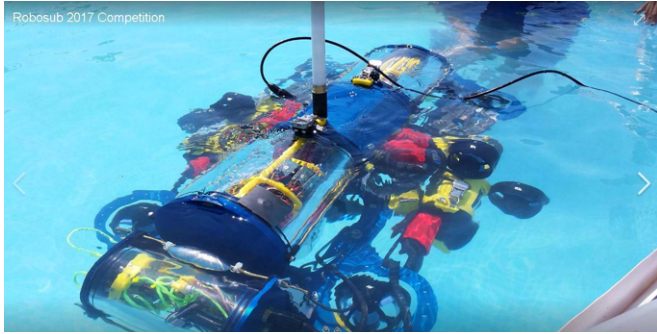
Additional Photos -

Vertical 3-Axis CNC machining and
waterjet cut components



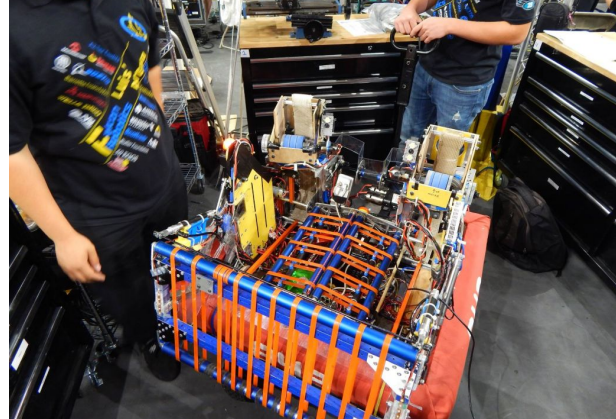
Carl Hayden Falcon Robotics -

Additional Photos -



Carl Hayden Falcon Robotics -

Additional Photos -



Project Two (100 points): A notched, rectangular cross-section cantilever beam is loaded in bending ($F = 50$ lb). Determine a reasonable finite element mesh and compare its prediction of maximum stress and deflection with a closed form solution for the points at the beam end (deflection), at point D (max stress) and at the location of notch (max stress). A 2D plane stress finite element model is assumed.

The beam dimensions in Figure 1 are: $a = 4$ in, $d = 7.5$ in, $l = 10$ in, $b = 0.1$ in, $h = 1$ in, and $r = 0.167$ in. The material is steel ($E = 30 \times 10^6$ psi). The supporting wall is considered to be much stiffer than the beam. Beam weight is negligible compared to the applied load. At the notch the stress concentration factor $K_t = 1.56$. Four different levels of mesh should be considered. Calculate (i) the maximum deflection and (ii) the stress values at point D and at the notch for each of these mesh conditions and compare them with the analytical values through a table. Plot the mesh convergence for the deflection at the tip and the stresses at points D and A. Which one converges faster and why? Compare the maximum Von Mises stresses with the theoretical value.

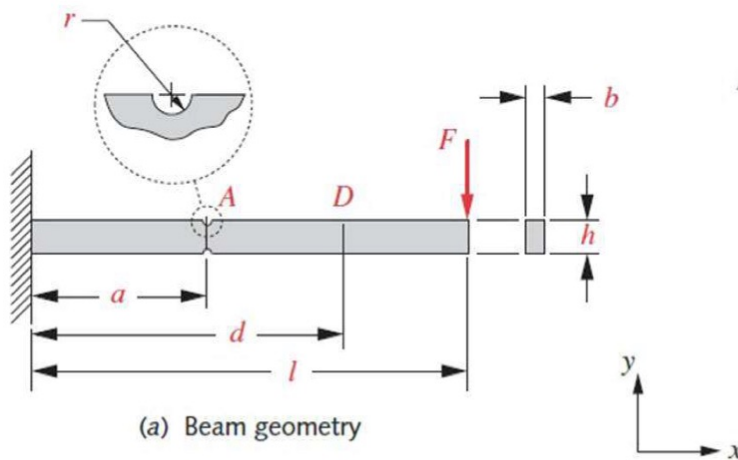


Figure 1

Analytical Solution to notched beam

$$r = 0.167 \text{ in.}$$

$$a = 4 \text{ in.}$$

$$d = 7.5 \text{ in}$$

$$F = 50 \text{ N}$$

$$l = 10 \text{ in}$$

$$h = 1 \text{ in}$$

$$b = 0.1 \text{ in.}$$

$$K \text{ at notch} = 1.56 \text{ given}$$

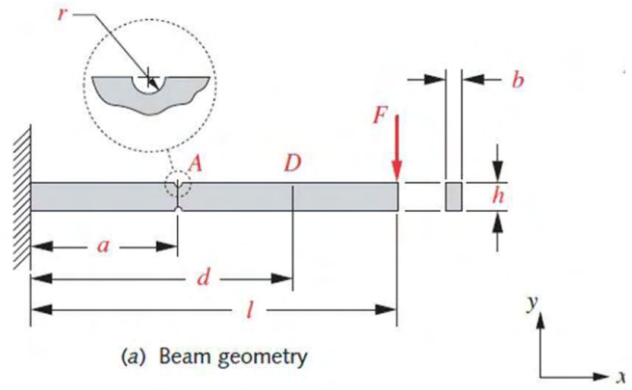
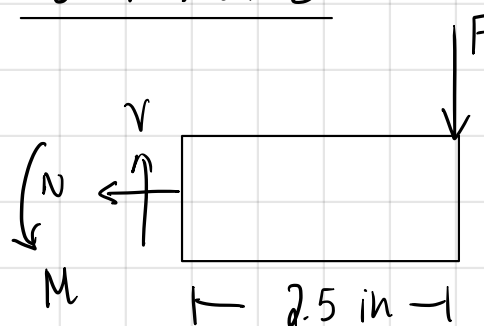


Figure 1

$$E = 30 \text{ MPa}$$

Section at D



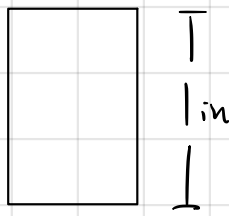
$$\sum F_x = 0 \rightarrow N = 0$$

$$\sum F_y = 0 \rightarrow F = V$$

$$\sum M_{\text{section}} = 0 \rightarrow -F(2.5) + M = 0$$

$$M_D = 125$$

$$\text{Stress at D} \Rightarrow \sigma = \frac{M_D Y}{I}$$

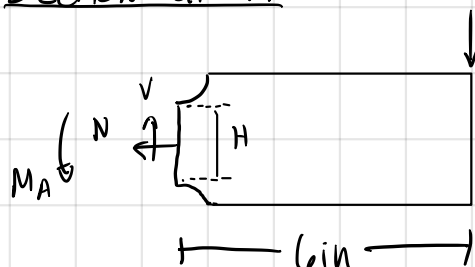


$$y = 0.5 \text{ in}$$

$$I = \frac{1}{12} (.1)(1)^3 = 8.33 \times 10^{-3}$$

$$\sigma = \frac{125(0.5)}{I} \Rightarrow 7.5 \text{ ksi}$$

Section at A



$$N = 0 \quad V = F$$

$$\sum M_A = 0 \quad F(6) = M$$

$$\sigma_A = \frac{300(H/2)}{I_A}$$

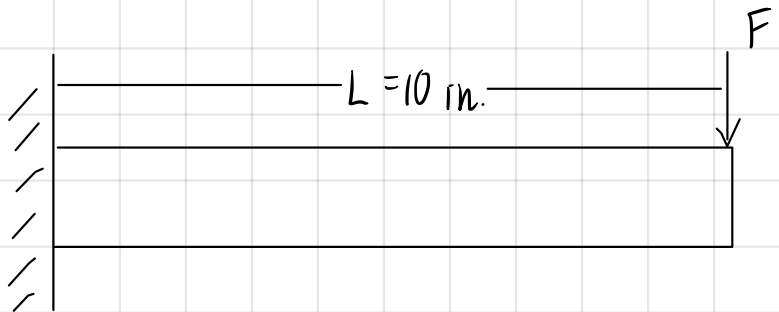


$$H = \frac{2}{3} \text{ in.}$$

$$I_A = \frac{1}{12} (0.1)(H)^3 \Rightarrow \frac{1}{12} (0.1)\left(\frac{2}{3}\right)^3 = 2.469 \times 10^{-3}$$

$$\sigma = 40.5 \text{ ksi} \rightarrow \text{apply stress concentration Factor}$$

$$K_C = 63.18 \text{ ksi}$$



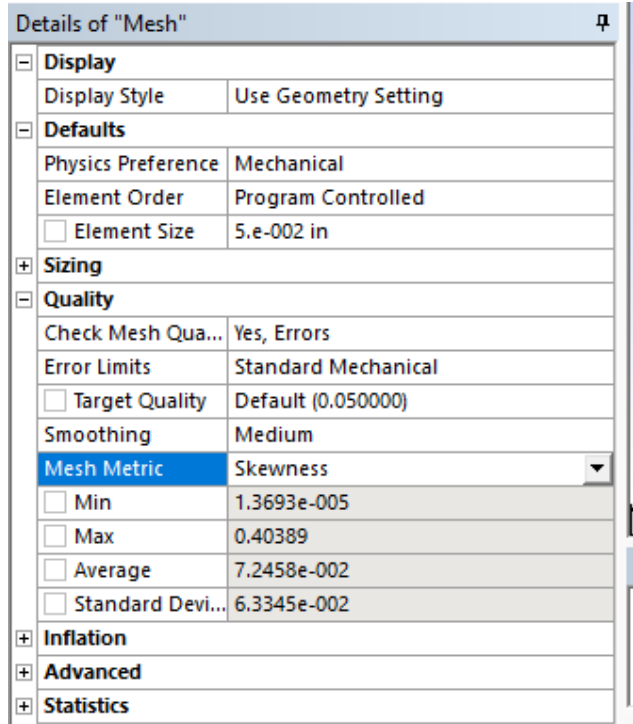
Max deflection for a cantilever beam $\Rightarrow \delta = \frac{FL^3}{3EI}$

$$\delta = \frac{50(10)^3}{3(30 \times 10^6)(8.333 \times 10^{-3})} = 0.06667 \text{ in.}$$

Study	Mesh size(in.)	# of nodes	Deflection at tip (in.)	Stress at D (Psi.)	Deflect. At D (in.)	Stress at A (Psi.)	Deflect. at A (in.)
Tri. Quad.	0.025	56503	0.074524	7499.9	0.046929	65278	0.014233
	0.05	18543	0.074489	7501.1	0.046924	64159	0.014232
	0.10	4507	0.074427	7502.6	0.046901	67914	0.014228
	0.15	2245	0.074382	7496.6	0.046886	68101	0.014226
	0.20	1523	0.074360	7498.6	0.046878	67717	0.014226
	0.25	1025	0.074321	7517.9	0.046853	66417	0.014214
Quadril linear	0.05	4219	0.074230	7546.7	0.046785	62065	0.014227
	0.10	1121	0.073597	7573.6	0.046426	57238	0.014217
	0.15	586	0.073468	7420.7	0.046357	55316	0.014212
	0.20	371	0.073334	7442.8	0.046283	55174	0.014202
	0.25	271	0.073319	7720	0.046275	54567	0.014191
Quadril Quad	0.05	12442	0.074512	7500	0.046927	62716	0.014232
	0.10	3249	0.074464	7500.1	0.046912	64075	0.014231
	0.15	1686	0.074438	7500	0.046905	63724	0.014229
	0.20	1048	0.074413	7500.5	0.046895	62136	0.014226
	0.25	775	0.074406	7500.2	0.046895	67604	0.014223

Comments:

I have chosen triangular quadratic element study because the data follows the analytical solution the closest. By choosing this study it also saves time from analyzing different mesh sizes and money compared to quadrilateral quadratic. Quadrilateral linear does not seem like a good choice in this situation since the order of the mesh is linear it has less integration points per node. The skewness from a mesh size of 0.05 in. in the triangle quadratic method yields an average value of 0.007246 which is really good. The mesh size of 0.05 in. comes from a mesh convergence and stress singularity study stated in the figures below.



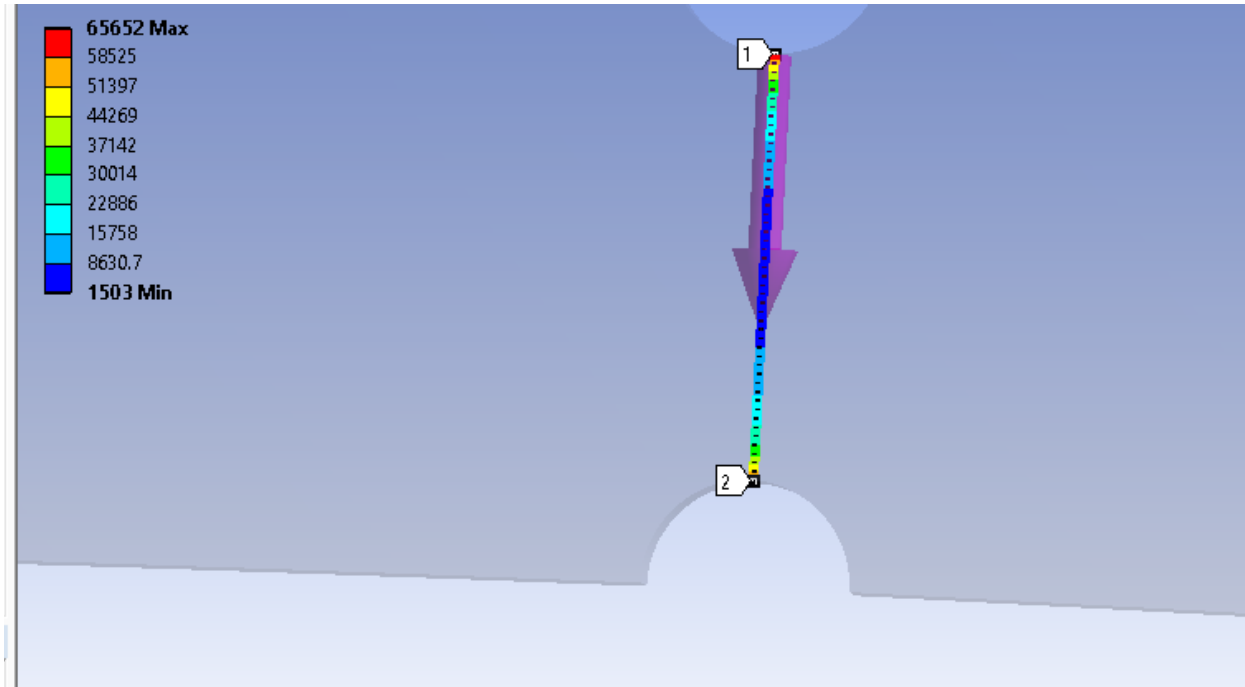
Checking for Stress Singularity at the notch

Sphere radius(in.)	Element size(in.)	Equivalent Stress at A (Psi)
.25	.100	63349
.20	.075	63999
.15	.050	65372
.10	.025	65050
.10	.010	65652

Comments:

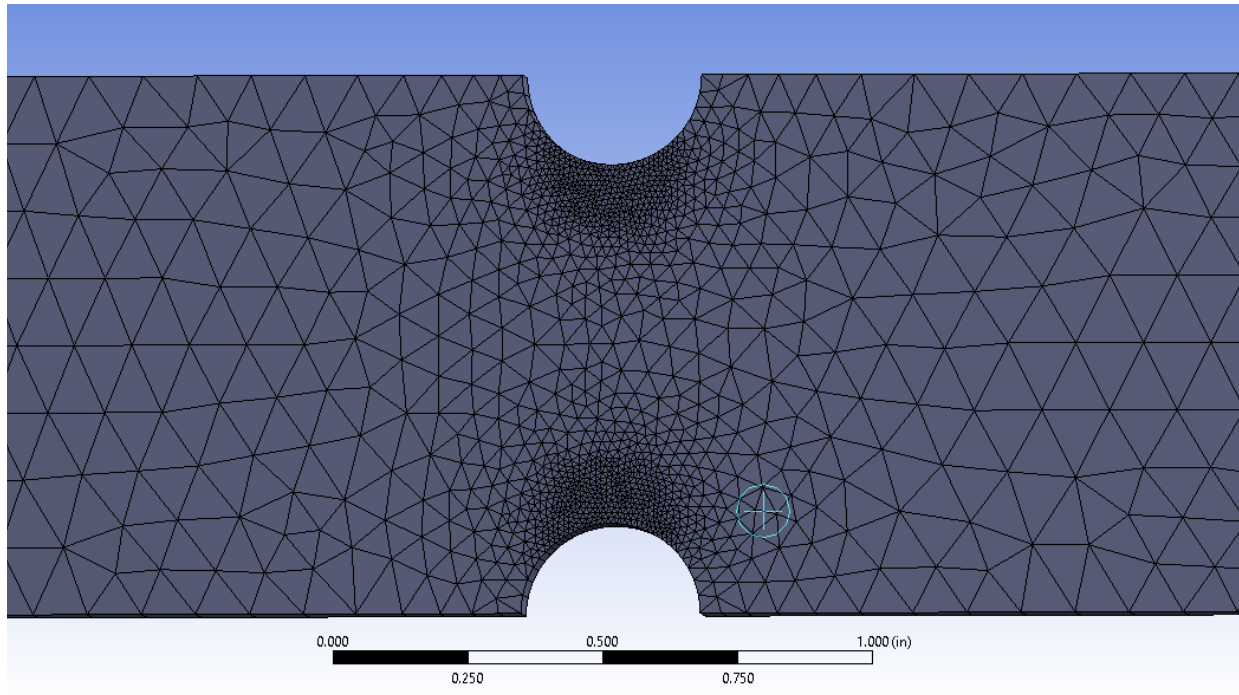
Even though the size of the element is approaching very small values at the point A the stress doesn't grow to infinity. Since there is no growth to infinity at the notch area we can conclude that there is no stress singularity at the notch.

Path which gives the max stress at point A.



This image shows how a sphere of influence was used to create a fine mesh at the notches.





Checking for Stress Singularity at the Tip

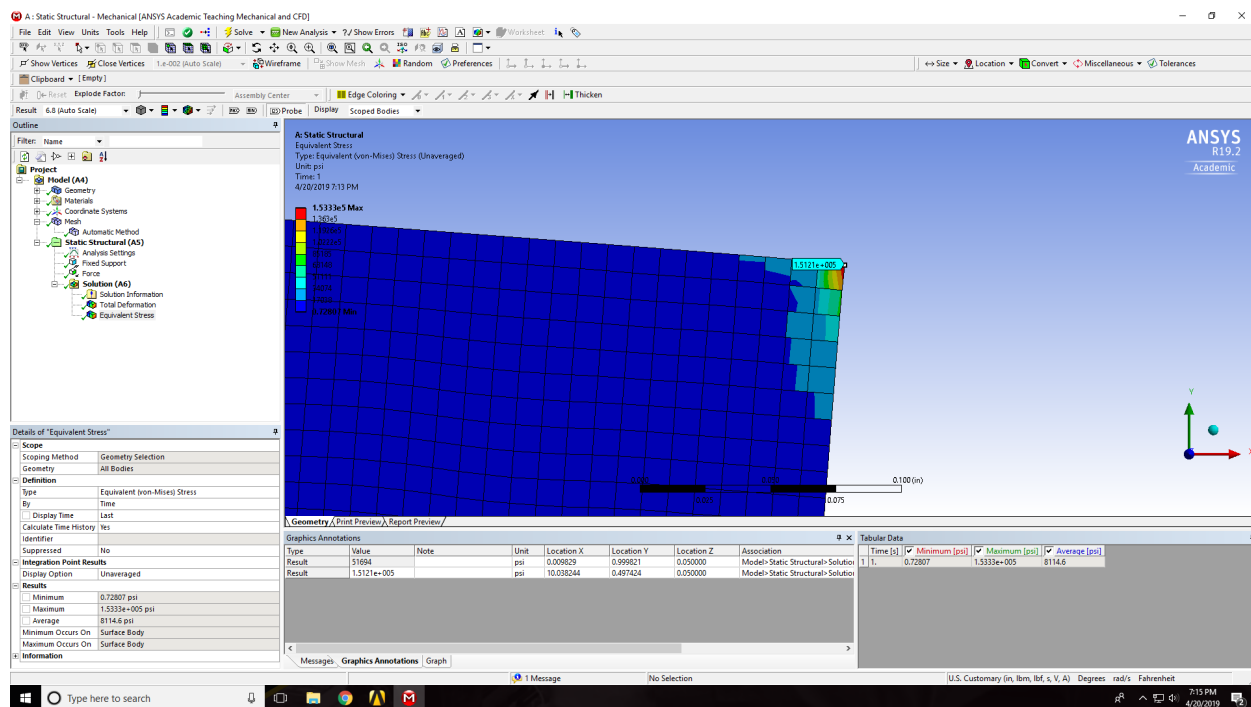
Sphere radius(in.)	Element size(in.)	Equivalent Stress at Tip (Psi)
.25	.100	29,197
.20	.075	39,312
.15	.050	51,011
.10	.025	107,690
.10	.010	309,690

Comments:

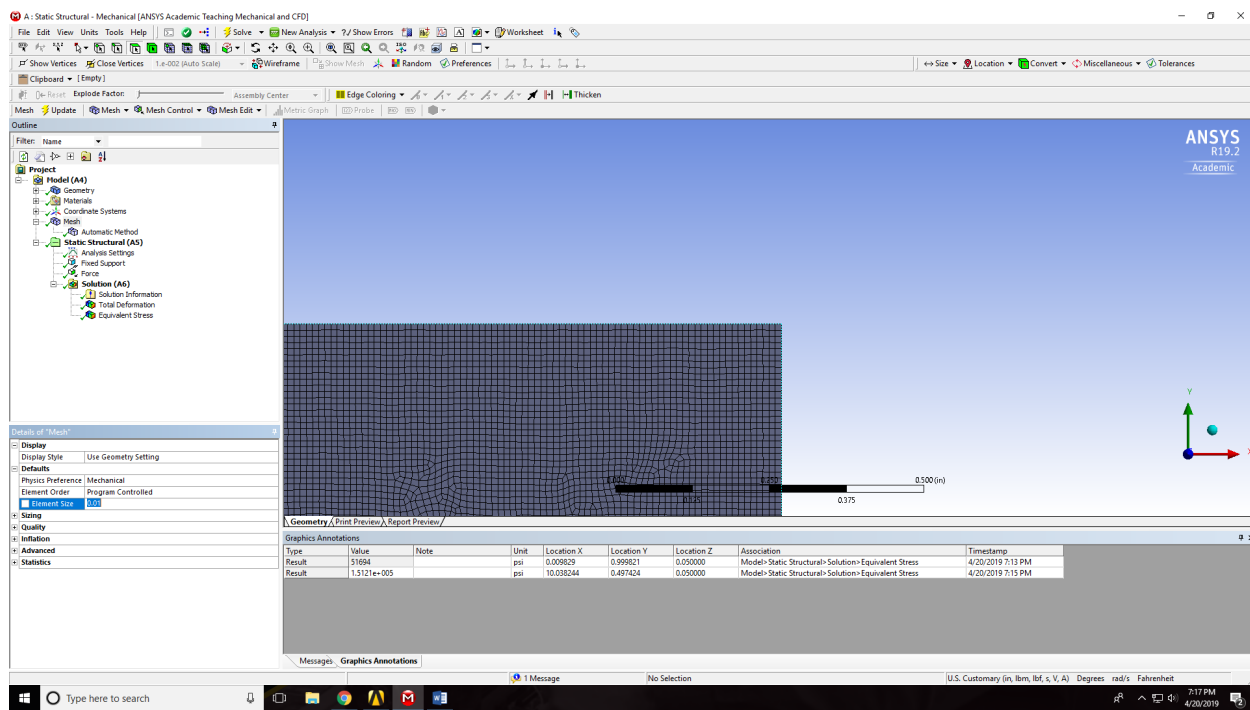
A sphere of interest was placed at the tip of the notched cantilever beam to run a stress singularity study. Every iteration the radius of the sphere at tip would decrease and so would

the element size, this allows us to ‘zoom in’ to the point of interest and create a really fine mesh at that location so we could really see what is going on. As you can see from the chart above there is a stress singularity occurring at the tip. Since the stress values become really large before 0.05 in. then that size of mesh will be our limiting factor.

Stress singularity at element size = 0.01 in.



Element size at which stress singularity occurs



From the graphs shown below it appears that the stress at D converges faster than the stress at A and the deflection at the tip. Within a few changes of the element size the stress at D approaches the analytical value while the other two need small mesh sizes to converge. This might be caused by the distance that D is located, it is far enough from the stress concentration at the notch and far from the singularity due to the force being applied at the tip.

Max Stresses vs analytical values.

Study	Mesh size(in.)	Analytical def. at tip (in.)	Deflection at tip (in.)	Stress at D (Psi.)	Analytical Stress at D (psi.)	Stress at A (Psi.)	Analytical stress at A (psi.)
Tri. Quad.	0.025	0.0666	0.074524	7499.9	7500	65278	63180
	0.05	0.0666	0.074489	7501.1	7500	64159	63180
	0.10	0.0666	0.074427	7502.6	7500	67914	63180
	0.15	0.0666	0.074382	7496.6	7500	68101	63180
	0.20	0.0666	0.074360	7498.6	7500	67717	63180
	0.25	0.0666	0.074321	7517.9	7500	66417	63180

```

clear all
% MEE 323 Project spring 2019
% Armando Chavez
% triangular quadratic
% num of nodes
N = [56503 18543 4507 2245 1523 1025];

% tot deflection
def_tot = [0.074524 0.074489 0.074427 0.074382 0.074360 0.074321];

% Stress at D
D = [7499.9 7501.1 7502.6 7496.6 7498.6 7517.9];

% Stress at notch A
A = [65278 64159 67914 68101 67717 66417];

figure (1)
plot(N,def_tot),title('Deflection at tip vs. Nodes')
xlabel('# of nodes'),ylabel('Deflection at tip(in.)')

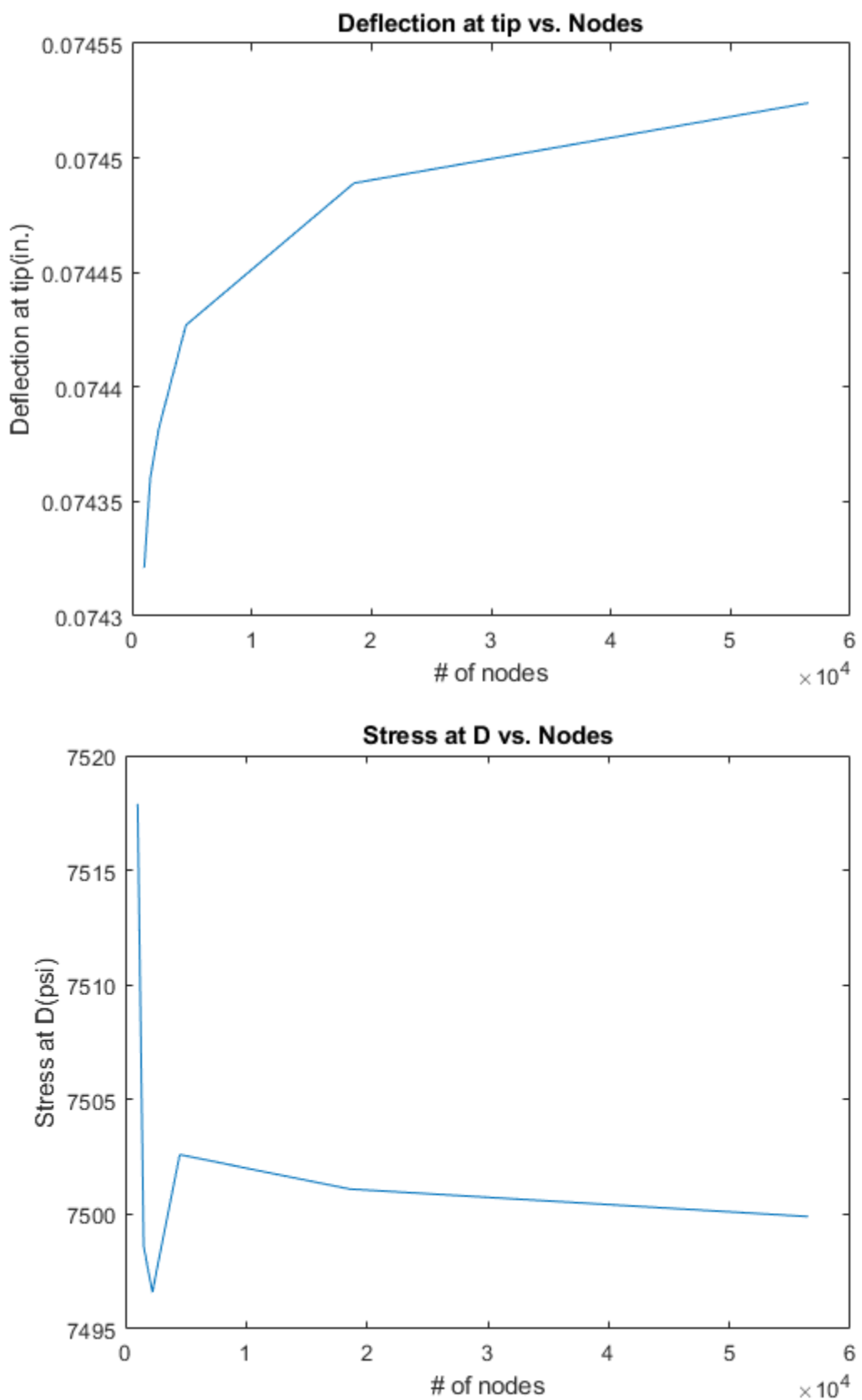
figure (2)
plot(N,D),title('Stress at D vs. Nodes')
xlabel('# of nodes'),ylabel('Stress at D(psi)')

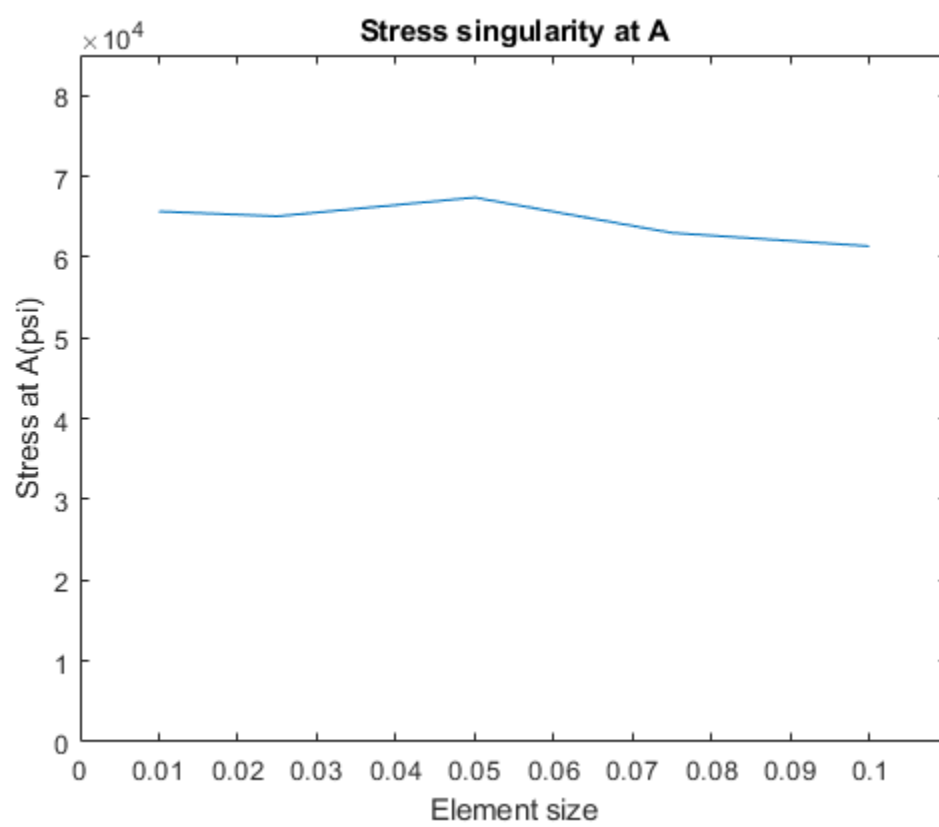
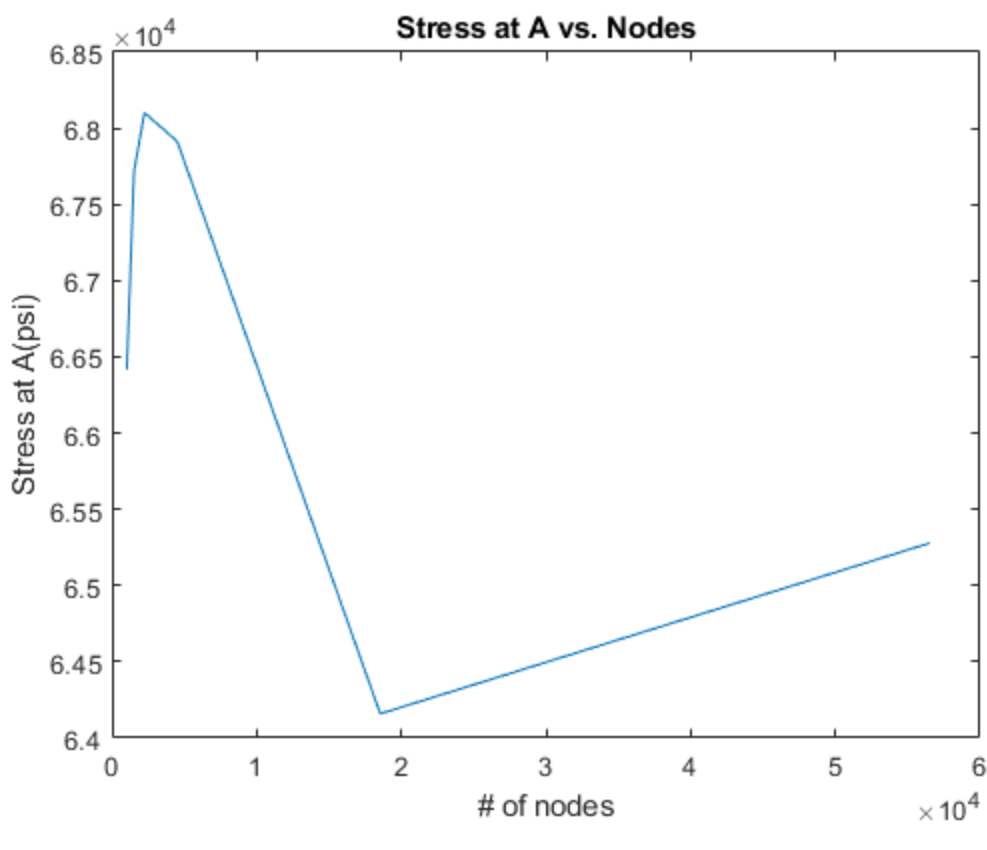
figure (3)
plot(N,A),title('Stress at A vs. Nodes')
xlabel('# of nodes'),ylabel('Stress at A(psi)')

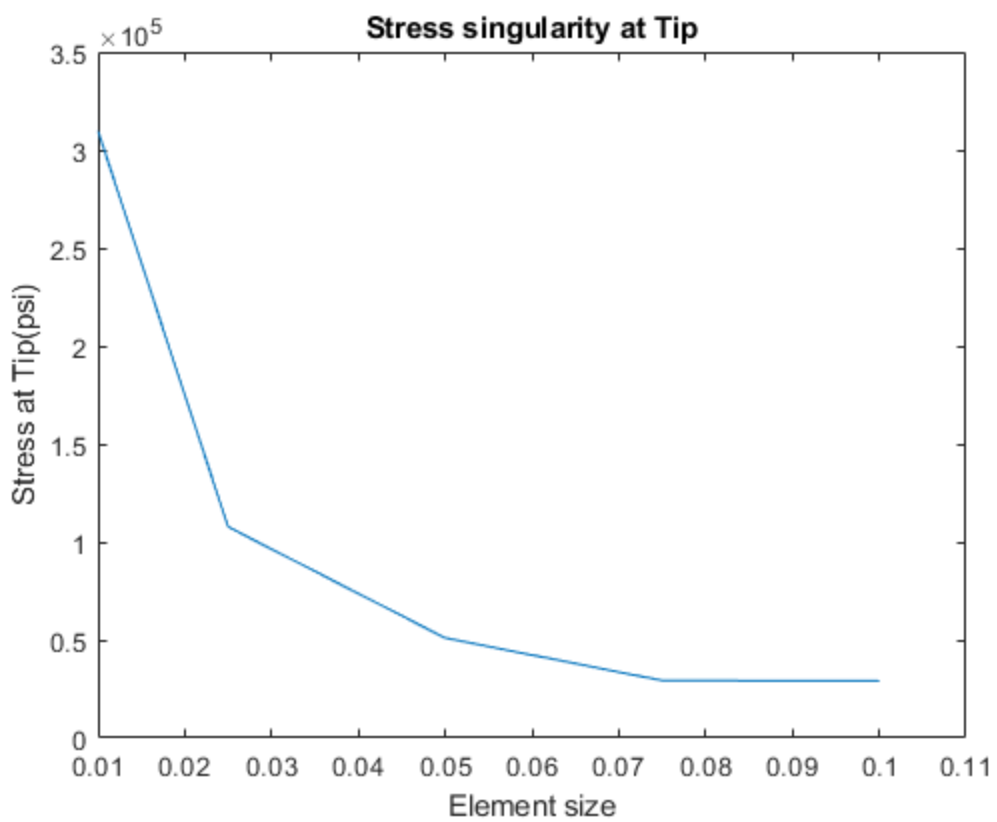
% Stress Singularity Check
% element size at notch A
sizeA = [.1 .075 .05 .025 .01];
% stress at A
stressA = [61349 62999 67372 65050 65652];
figure (4)
plot(sizeA,stressA),title('Stress singularity at A')
xlabel('Element size'),ylabel('Stress at A(psi)')
axis([0 .11 0 85000])

% element size at tip
sizeT = [.1 .075 .05 .025 .01];
% stress at tip
stressT = [29197 29312 51011 107690 309690];
figure(5)
plot(sizeT,stressT),title('Stress singularity at Tip')
xlabel('Element size'),ylabel('Stress at Tip(psi)')

```







Published with MATLAB® R2018a

Project: Figure 1 shows the engine mounted on a base with its output shaft connected via a clutch to the input shaft of a gearbox. The gearbox contains a single gearset to reduce the high engine speed. The output shaft has the larger torque which is defined as shown in Figure 2(a). In addition to the torque on the shafts, there are loads from gears that apply bending moments to the shaft.

The torque-time function on the output shaft is given in figure 2(a). The required gear ratio is a 3:1 reduction in velocity from the input to the output shaft. The diameters of the input and output gears are 4 in and 12 in, respectively. Both gears have the same thickness and 20° pressure angle as shown in Figure 2(b). We assume that the gears are centered between the simply supported bearings that are set 6 in apart. A stress concentration factor of 3 (for static force) for both bending and torsion at the critical location where both moment and torque are largest is assumed. Low – carbon cold-rolled steel SAE 1018 ($S_{ut} = 64$ ksi and $S_y = 54$ ksi) is considered for the design. Also assume the followings: (i) Machined finish; (ii) 50% reliability; (iii) notch radius of 0.01 in; and (iv) safety factor of 2.5 to account for the uncertainties.

- (a) Determine reasonable sizes for the input and output shafts of the gearbox considering the following failure criteria (i) Goodman (ii) Gerber (iii) ASME elliptic, and (iv) Soderberg. Summarize the results in a table and discuss.
- (b) Draw the fatigue diagram for input and output shafts with various criteria of failure including the load lines (use the diameters of the input and output shafts from Soderberg criterion in part a)

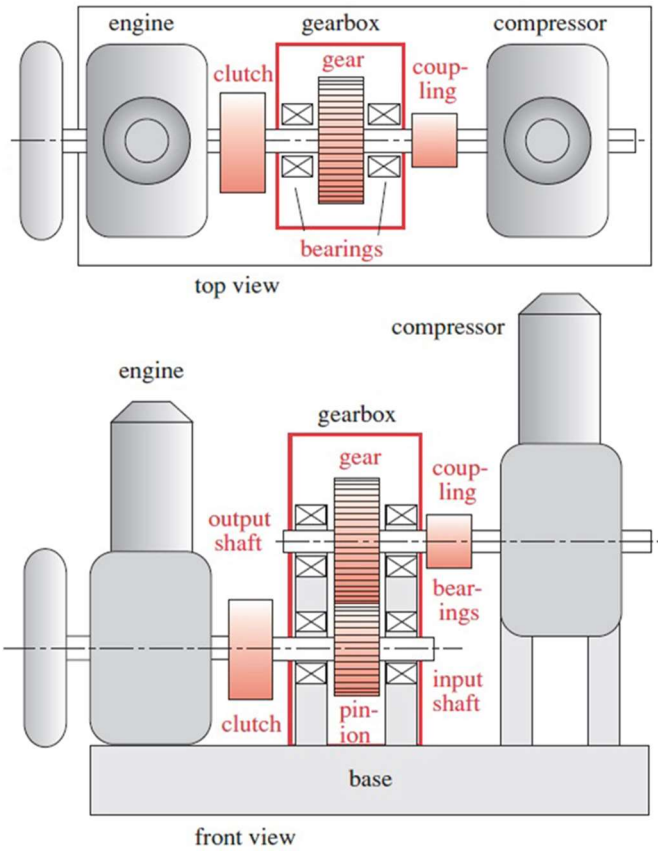
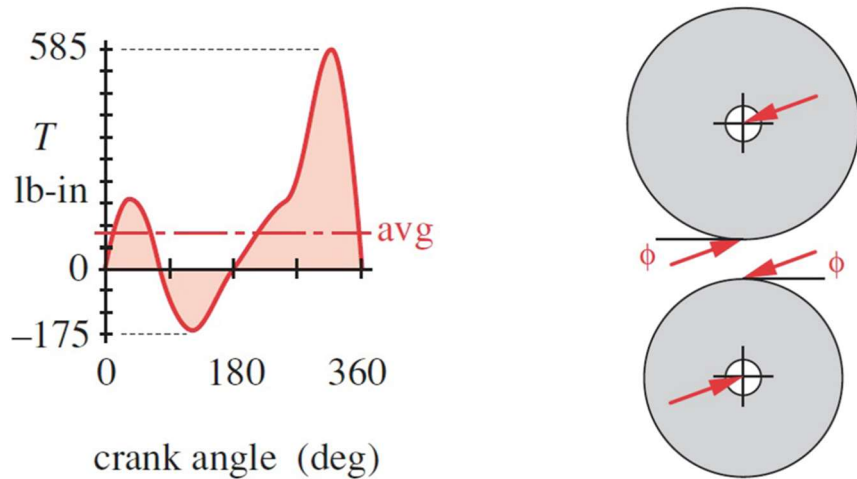


Figure 1. Preliminary design

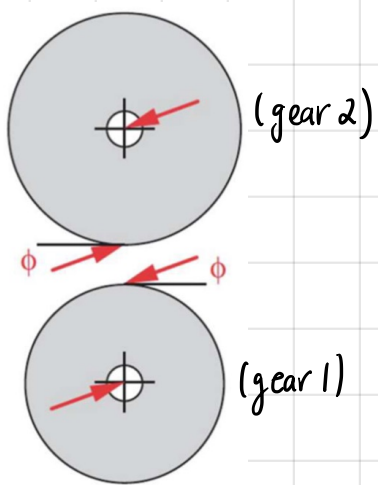


(a)

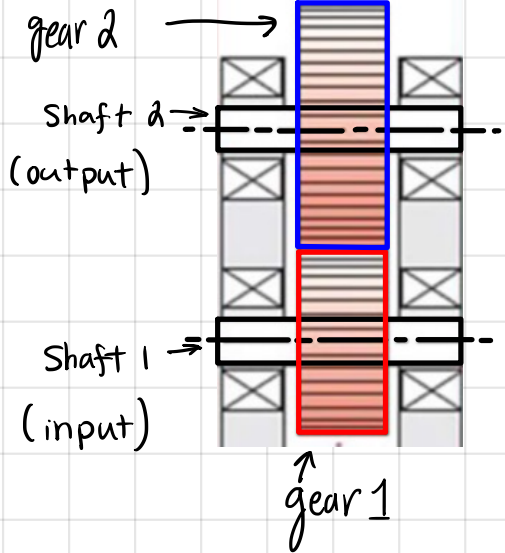
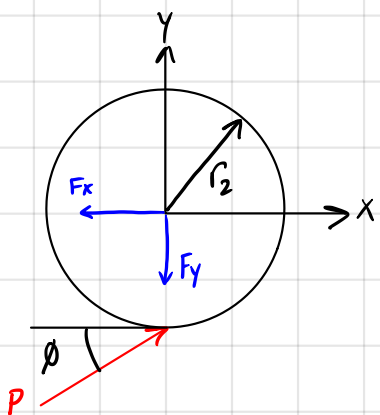
(b)

Figure 2. (a) Total torque-time function, (b) Forces on a Gearset ($\phi = 20^\circ$ pressure angle)

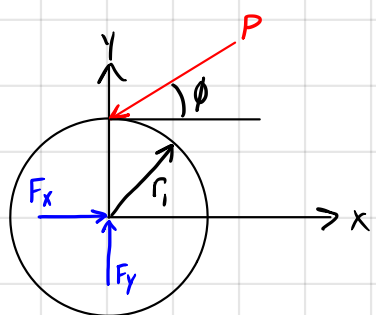
gear radius: $r_1 = 2 \text{ in}$, $r_2 = 6 \text{ in.}$, $\phi = 20^\circ$



FBD 2:



FBD 1:



FBD 1:

$$\sum F_x = 0 \Rightarrow -P \cos \phi + F_x = 0 \quad F_x = P \cos \phi \quad \left. \begin{array}{l} \\ \end{array} \right\} * \text{Same for FBD 2}$$

$$\sum F_y = 0 \Rightarrow -P \sin \phi + F_y = 0 \quad F_y = P \sin \phi$$

$$\sum M_z = 0 \Rightarrow P \cos \phi \cdot r_1 - T_1 = 0 \quad \frac{T_1 = P \cos \phi \cdot r_1}{T_1 = P \cos \phi \cdot r_1} \quad (\text{eq. 1})$$

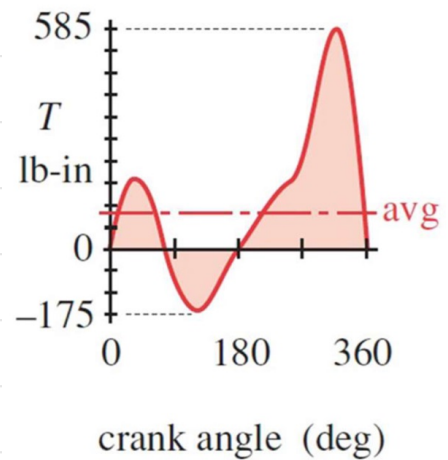
FBD 2:

$$\sum M_z = 0 \Rightarrow P \cos \phi \cdot r_2 - T_2 = 0 \quad \frac{T_2 = P \cos \phi \cdot r_2}{T_2 = P \cos \phi \cdot r_2} \quad (\text{eq. 2})$$

* The graph to the right shows torque in the output shaft which I have labeled as shaft number 2 in the previous part

$$(T_2)_{\max} = 585 \text{ lb-in} \rightarrow 585 = P \cos(20)(6 \text{ in}) \rightarrow P_{\max} = 103.75 \text{ lb}$$

$$(T_2)_{\min} = -175 \text{ lb-in} \rightarrow -175 = P \cos(20)(6 \text{ in}) \rightarrow P_{\min} = -31.04 \text{ lb}$$



crank angle (deg)

$$P_{\text{alternate}} = \frac{P_{\max} - P_{\min}}{2} = \frac{(103.75) - (-31.04)}{2} = 67.4 \text{ lb.}$$

$$P_{\text{midrange}} = \frac{P_{\max} + P_{\min}}{2} = \frac{(103.75) + (-31.04)}{2} = 36.36 \text{ lb.}$$

* These will be the same values for both shafts since the reactions from above are equal, however T_a and T_m will not be the same for both shafts.

$$(T_2)_{\max} = 585 \text{ lb-in} \quad (T_2)_a = \frac{585 - (-175)}{2} = \frac{380}{2} \text{ lb-in}$$

$$(T_2)_{\min} = -175 \text{ lb-in} \quad (T_2)_m = \frac{585 + (-175)}{2} = \frac{205}{2} \text{ lb-in}$$

From (eq.1) $\rightarrow T_1 = P \cos \phi \cdot r_1$

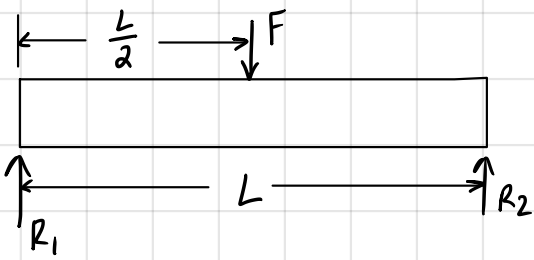
$$(T_1)_{\max} = P_{\max} \cos \phi \cdot r_1 = (103.75 \text{ lb}) \cos(20^\circ)(2 \text{ in}) = 195 \text{ lb-in}$$

$$(T_1)_{\min} = P_{\min} \cos \phi \cdot r_1 = (-31.04 \text{ lb}) \cos(20^\circ)(2 \text{ in}) = -58.333 \text{ lb-in}$$

$$(T_1)_a = \frac{195 - (-58.333)}{2} = \frac{126.667}{2} \text{ lb-in}$$

$$(T_1)_m = \frac{195 + (-58.333)}{2} = \frac{68.333}{2} \text{ lb-in}$$

* Solving for $(T_1)_a$ and $(T_1)_m$ could have been solved easier by dividing $(T_2)_a$ and $(T_2)_m$ by the gear ratio.



* on a simple supported structure like this one the max bending occurs at the center where the force is located
 So $M_{\max} = \frac{F}{2} (L/2)$
 - in this case $L = 6 \text{ in}$.

$$M_a = \frac{P_a \cdot d}{2} = \frac{(67.4 \text{ lb})(3 \text{ in})}{2} = 101.1 \text{ lb-in} \quad - \text{Also } d = \frac{L}{2} = 3 \text{ in.}$$

$$M_m = \frac{P_m \cdot d}{2} = \frac{(36.36 \text{ lb})(3 \text{ in})}{2} = 54.54 \text{ lb-in}$$

* M_a and M_m can be used for both shafts from FBD's

For shaft 1

$$M_a = 101.1 \text{ lb-in}$$

$$M_m = 54.54 \text{ lb-in}$$

$$(T_1)_a = 126.667 \text{ lb-in}$$

$$(T_1)_m = 68.333 \text{ lb-in}$$

$$\sigma = \frac{My}{I} = \frac{M(\frac{D}{2})}{\frac{\pi}{32}(\frac{D}{2})^3} = \frac{32M}{\pi D^3}$$

$$\tau = \frac{T_r}{J} = \frac{T(\frac{D}{2})}{\frac{\pi}{16}(\frac{D}{2})^3} = \frac{16T}{\pi D^3}$$

$$\sigma_a = \frac{32(101.1)}{\pi D_1^3} = \frac{1029.8}{D_1^3}$$

$$\tau_{a,1} = \frac{16(126.667)}{\pi D_1^3} = \frac{645.1}{D_1^3}$$

$$\sigma_m = \frac{32(54.54)}{\pi D_1^3} = \frac{555.54}{D_1^3}$$

$$\tau_{m,1} = \frac{16(68.333)}{\pi D_1^3} = \frac{348.02}{D_1^3}$$

$$\sigma'_a = \left\{ \left[K_f \sigma_{Bend} + \frac{K_f \sigma_{Axial}}{0.85} \right]^2 + 3 \left[K_{fs} (\tau_a) \right]^2 \right\}^{1/2}$$

$$K = K_s = 3$$

notch radius $r = 0.01 \text{ in}$

$$\sigma'_m = \left\{ \left[K_{fm} (\sigma_m)_{Bend} + K_f (\sigma_m)_{Axial} \right]^2 + 3 [K_{fs} \tau_m]^2 \right\}^{1/2}$$

Bending or axial: $\sqrt{a} = 0.246 - 3.08(10^{-3})S_{ut} + 1.51(10^{-5})S_{ut}^2 - 2.67(10^{-8})S_{ut}^3$ (6-35a)

Torsion: $\sqrt{a} = 0.190 - 2.51(10^{-3})S_{ut} + 1.35(10^{-5})S_{ut}^2 - 2.67(10^{-8})S_{ut}^3$ (6-35b)

$$(\sqrt{a})_{Bending} = 0.246 - 3.08 \times 10^{-3}(64) + 1.51 \times 10^{-5}(64^2) - 2.67 \times 10^{-8}(64)^3 = 0.10373$$

$$(\sqrt{a})_{Torsion} = 0.190 - 2.51 \times 10^{-3}(64) + 1.35 \times 10^{-5}(64^2) - 2.67 \times 10^{-8}(64)^3 = 0.07765$$

$$q = \frac{1}{1 + \frac{0.10373}{\sqrt{0.01}}} = 0.563 \quad q_s = \frac{1}{1 + \frac{0.07765}{\sqrt{0.01}}} = 0.491$$

$$q = \frac{1}{1 + \frac{\sqrt{a}}{\sqrt{r}}}$$

$$q_s = 0.563, \quad q = 0.491$$

$$k_f = q_s(k-1) + 1 = 0.491(3-1) + 1 = 1.98$$

$$k_{fs} = q_s(k_s-1) + 1 = 0.5(3-1) + 1 = 2.126$$

Mod-Goodman eq.

$$\frac{\sigma_A}{S_e} + \frac{\sigma_m}{S_{ut}} = \frac{1}{n}$$

$$n = 2.5 \quad S_{ut} = 64 \text{ kpsi}$$

$$S_e = K_A K_B K_C K_O K_E \dots S'_e$$

$$S'_e = \begin{cases} 0.5 S_{ut} & S_{ut} \leq 200 \text{ kpsi (1400 MPa)} \\ 100 \text{ kpsi} & S_{ut} > \text{kpsi} \\ 700 \text{ MPa} & S_{ut} > 1400 \text{ MPa} \end{cases}$$

$$K_A = a S_{ut}^b \quad , \text{ machined Surface}$$

$$S'_e = 0.5 S_{ut} = 32 \text{ kpsi}$$

$$\text{From table 6.2 } a = 2.7, b = -0.265 \rightarrow 2.7(64)^{-0.265} = \underline{0.896 = K_A}$$

K_B , Size factor assume: d is in the range $0.11 \leq d \leq 2 \text{ in}$, this range yields an equation:

$$K_B = 0.879 d^{-0.107} \quad , \text{ assume } d = 1 \text{ in} \rightarrow \underline{K_B = 0.879}$$

K_C , loading Factor $\rightarrow \underline{K_C = 1}$, for combined loading

K_D , Temperature factor $\underline{K_D = 1}$, no information give so K_D is taken as 1

K_E , Reliability Factor, From table 6.5 @ 50% reliability $\underline{K_E = 1}$

$$S_e = (0.896)(0.879)(1)(1)(1)(32 \text{ kpsi}) = 25.2 \text{ kpsi}$$

For this First iteration Dowling method will not be considered

$$K_f = K_{fm} = 1.98$$

$$\sigma_{A,\text{axial}} = 0$$

$$K_{fs} = K_{fsm} = 2.126$$

$$\sigma'_a = \left\{ \left[K_f \sigma_{a,\text{bend}} + \frac{K_f \sigma_{A,\text{axial}}}{0.85} \right]^2 + 3 \left[K_{fs} (\tau_a) \right]^2 \right\}^{1/2}$$

$$\sigma'_m = \left\{ \left[K_{fm} (\sigma_m)_{\text{bend}} + K_f (\sigma_m)_{\text{axial}} \right]^2 + 3 [K_{fsm} \tau_m]^2 \right\}^{1/2}$$

$$\sigma_{A,\text{Bend}} = \frac{1029.8}{(1)^3} = 1029.8 \text{ psi}$$

$$\tau_{a,1} = 645.1$$

$$\sigma_{m,\text{Bend}} = 555.54 \text{ psi}$$

$$\tau_{m,1} = 348.02$$

$$\sigma_a' = \left\{ [(1.98)(1029.8)]^2 + 3[(2.126)(645.1)]^2 \right\}^{1/2} = 3.13 \text{ kpsi}$$

$$\sigma_m' = \left\{ [(1.98)(555.54)]^2 + 3[(2.126)(348.02)]^2 \right\}^{1/2} = 1.43 \text{ kpsi}$$

$$\frac{3.13 \text{ kpsi}}{25.2 \text{ kpsi}} + \frac{1.43 \text{ kpsi}}{64 \text{ kpsi}} = \frac{1}{2.5} \Rightarrow 6.82 \neq 2.5$$

* Second iteration, assume $d = 0.5 \text{ in.}$

$$K_A = 0.896 \quad K_B = 0.879 d^{-0.107} \quad 0.11 \leq d \leq 2 \text{ in.}$$

$$K_C = 1 \quad = 0.946$$

$$K_D = 1$$

$$K_E = 1 \rightarrow S_e = (.896)(.946)32 \text{ ksi} = 27.123 \text{ ksi}$$

$$S_e' = 32 \text{ ksi}$$

$$\sigma_a = \frac{1029.8}{D_i^3} = \frac{1,029.8}{(0.5)^3} = 8.238 \text{ ksi} \quad T_{a,1} = \frac{645.1}{D_i^3} = \frac{645.1}{(0.5)^3} = 5.161 \text{ ksi}$$

$$\sigma_m = \frac{555.54}{D_i^3} = \frac{555.54}{(0.5)^3} = 4.444 \text{ ksi} \quad T_{m,1} = \frac{348.02}{D_i^3} = \frac{348.02}{0.5^3} = 2.784 \text{ ksi}$$

$$\sigma_a' = \left\{ [(1.98)(8.238)]^2 + 3[(2.126)(5.161)]^2 \right\}^{1/2} = 25.04 \text{ ksi}$$

$$\sigma_m' = \left\{ [(1.98)(4.444)]^2 + 3[(2.126)(2.784)]^2 \right\}^{1/2} = 13.51 \text{ ksi}$$

$$\frac{25.04}{27.123} + \frac{13.51}{64} = \frac{1}{2.5} \Rightarrow 0.881 \neq 2.5$$

* 3rd iteration, assume $d = 0.75 \text{ in.}$

$$K_A = 0.896, K_C = 1, K_D = 1, K_E = 1, K_B = 0.879 d^{-0.107} \quad 0.11 \leq d \leq 2 \text{ in.}$$

$$S_e' = 32 \text{ ksi} \quad = 0.879(.75)^{-0.107} = 0.906$$

$$\rightarrow S_e = (.896)(.906)32 \text{ ksi} = 25.98 \text{ ksi}$$

$$\sigma_a = \frac{1029.8}{D_i^3} = \frac{1,029.8}{(0.75)^3} = 2.441 \text{ ksi} \quad T_{a,1} = \frac{645.1}{D_i^3} = \frac{645.1}{(0.75)^3} = 1.529 \text{ ksi}$$

$$\sigma_m = \frac{555.54}{D_i^3} = \frac{555.54}{(0.75)^3} = 1.317 \text{ ksi} \quad T_{m,1} = \frac{348.02}{D_i^3} = \frac{348.02}{(0.75)^3} = 0.825 \text{ ksi}$$

$$\sigma_a' = \left\{ [(1.98)(2.441)]^2 + 3[(2.126)(1.529)]^2 \right\}^{1/2} = 7.420 \text{ ksi}$$

$$\sigma_m' = \left\{ [(1.98)(1.317)]^2 + 3[(2.126)(0.825)]^2 \right\}^{1/2} = 4.003 \text{ ksi}$$

$$\frac{7.420}{25.98} + \frac{4.003}{64} = \frac{1}{2.5} \Rightarrow 2.87 \neq 2.5$$

* 4th iteration, $d = 0.70 \text{ in}$

$$k_B = 0.879(0.7)^{-0.107} = .9132 \quad S_e = (.896)(.9132)(32) = 26.183 \text{ ksi}$$

$$\sigma_a = 3.002 \text{ ksi} \quad T_{a,1} = 1.8807 \text{ ksi} \quad \sigma_a' = 9.126 \text{ ksi}$$

$$\sigma_m = 1.6197 \text{ ksi} \quad T_{m,1} = 1.0146 \text{ ksi} \quad \sigma_m' = 4.92375 \text{ ksi}$$

$$\frac{9.126}{26.183} + \frac{4.92375}{64} = \frac{1}{n} \Rightarrow 2.35 \neq 2.5$$

* 5th iteration, $d = 0.725 \text{ in}$ $k_B = 0.879(0.725)^{-0.107} \rightarrow k_B = 0.9098$

$$S_e = (.896)(0.9098)(32) = 26.085 \text{ ksi}$$

$$\sigma_a = 2.702 \text{ ksi} \quad T_{a,1} = 1.693 \text{ ksi}$$

$$\sigma_m = 1.458 \text{ ksi} \quad T_{m,1} = 0.913 \text{ ksi}$$

$$\sigma_a' = 8.215 \text{ ksi}$$

$$\sigma_m' = 4.432 \text{ ksi}$$

$$\frac{8.215}{26.085} + \frac{4.432}{64} = \frac{1}{n} = 2.603 \neq 2.5$$

Since we are within 5% of final value
 $0.7 < d < 0.725 \text{ in.}$

DE-Goodman equation (Chap 7)

$$d = \left(\frac{16n}{\pi} \left\{ \frac{1}{S_e} [4(K_f M_a)^2 + 3(K_{fs} T_a)^2]^{1/2} + \frac{1}{S_{ut}} [4(K_f M_m)^2 + 3(K_{fs} T_m)^2]^{1/2} \right\} \right)^{1/3}$$

* 6th iteration: assume $d=0.725 \quad k_B = 0.879(0.725)^{-0.107} \rightarrow k_B = 0.9098$

$$S_e = (.9098)(.896)(32) = 26.085 \text{ ksi} \rightarrow d = 0.7153 \text{ in.}$$

* 7th iteration: assume $d=0.7153 \text{ in.}, k_B = 0.879(0.7153)^{-0.107} = 0.911$

$$S_e = (.896)(0.911)(32) = 26.12 \text{ ksi} \rightarrow d = 0.7150 \text{ in.}$$

Soderberg eq.

$$\frac{\sigma'_a}{S_e} + \frac{\sigma'_m}{S_y} = \frac{1}{n}, \quad S_y = 54 \text{ ksi}, \quad n = 2.5$$

1st iteration $d = 1.1\text{in.}$, $\sigma'_a = 3.13 \text{ kpsi}$, $\sigma'_m = 1.43 \text{ kpsi}$, $S_e = 27 \text{ ksi}$

$$\frac{3.13}{27} + \frac{1.43}{54} = \frac{1}{2.5} \Rightarrow 7.022 \neq 2.5$$

2nd iteration $d = 0.5$, $\sigma'_a = 25.04 \text{ ksi}$, $\sigma'_m = 13.51 \text{ ksi}$, $S_e = 27.123 \text{ ksi}$

$$\frac{25.04}{27.123} + \frac{13.51}{54} = \frac{1}{2.5} \Rightarrow 0.852 \neq 2.5$$

3rd iteration $d = 0.75$, $\sigma'_a = 7.420 \text{ ksi}$, $\sigma'_m = 4.003 \text{ ksi}$, $S_e = 25.98 \text{ ksi}$

$$\frac{7.42}{25.98} + \frac{4.003}{54} = \frac{1}{2.5} \Rightarrow 2.78 \neq 2.5$$

4th Iteration $d = 0.7$, $\sigma'_a = 9.126 \text{ ksi}$, $\sigma'_m = 4.92375 \text{ ksi}$, $S_e = 26.183 \text{ ksi}$

$$\frac{9.126}{26.183} + \frac{4.92375}{54} = \frac{1}{2.5} \Rightarrow 2.274 \neq 2.5$$

5th iteration $d = 0.725$, $\sigma'_a = 8.215 \text{ ksi}$, $\sigma'_m = 4.432 \text{ ksi}$, $S_e = 26.085 \text{ ksi}$

$$\frac{8.215}{26.085} + \frac{4.432}{54} = \frac{1}{2.5} \Rightarrow 2.518 \neq 2.5$$

* using the same shaft diameter from above but eqn from chap.7

$$d = \left(\frac{16n}{\pi} \left\{ \frac{1}{S_e} [4(K_f M_a)^2 + 3(K_{fs} T_a)^2]^{1/2} + \frac{1}{S_y} [4(K_f M_m)^2 + 3(K_{fs} T_m)^2]^{1/2} \right\} \right)^{1/3}$$

$$\Rightarrow d = .722$$

Iteration # 6 with $d = 0.722$

$$K_B = 0.879(0.722)^{-0.107} = 0.9102 \quad S_e = (1.896)(0.9102)(32) = 26.1 \text{ ksi}$$

$\Rightarrow d = 0.723$

DE - Gerber equation:

$$M_a = 101.1 \text{ lb.in}$$

$$K_f = 1.98$$

$$d = \left(\frac{8nA}{\pi S_e} \left\{ 1 + \left[1 + \left(\frac{2BS_e}{AS_{ut}} \right)^2 \right]^{1/2} \right\} \right)^{1/3}$$

$$M_m = 54.54 \text{ lb.in}$$

$$K_{fs} = 2.126$$

$$(T_a)_a = 126.667 \text{ lb.in}$$

$$h = 2.5$$

$$A = \sqrt{4(K_f M_a)^2 + 3(K_{fs} T_a)^2}$$

$$(T_m)_m = 68.333 \text{ lb.in}$$

$$S_{ut} = 64 \text{ ksi}$$

$$B = \sqrt{4(K_f M_m)^2 + 3(K_{fs} T_m)^2}$$

$$A = (4(1.98 \times 101.1)^2 + 3(2.126 \times 126.667)^2)^{1/2} = 614.69$$

$$B = (4(1.98 \times 54.54)^2 + 3(2.126 \times 68.333)^2)^{1/2} = 331.61$$

* 1st iteration, assume $d = 0.75 \text{ in.}$, $K_b = 0.879(0.75)^{-0.107} = .906$

$$S_e = (.896)(.906)(32) = 26 \text{ ksi} \rightarrow d = 0.679 \text{ in.}$$

* 2nd iteration, assume $d = 0.679 \text{ in.}$, $K_b = 0.879(0.679)^{-0.107} = 0.916$

$$S_e = (.896)(0.916)(32) = 26.269 \text{ psi} \rightarrow d = 0.677 \text{ in.}$$

DE - ASME Elliptic

$$d = \left\{ \frac{16n}{\pi} \left[4 \left(\frac{K_f M_a}{S_e} \right)^2 + 3 \left(\frac{K_{fs} T_a}{S_e} \right)^2 + 4 \left(\frac{K_f M_m}{S_y} \right)^2 + 3 \left(\frac{K_{fs} T_m}{S_y} \right)^2 \right]^{1/2} \right\}^{1/3}$$

* 1st iteration, assume $d = 0.75 \text{ in.}$, $K_b = 0.879(0.75)^{-0.107} = .906$, $S_y = 54 \text{ ksi}$

$$S_e = (.896)(.906)(32) = 26 \text{ ksi}, \text{ Plug } S_e \text{ into equation above}$$

$$\rightarrow d = 0.6775 \text{ in.}$$

* 2nd iteration, assume $d = 0.6775 \text{ in.}$, $K_b = 0.879(0.6775)^{-0.107} = 0.9164$

$$S_e = (.896)(0.9164)(32) = 26.275 \text{ ksi} \rightarrow d = 0.675 \text{ in.}$$

For shaft 2

Known information:

$$\begin{aligned}
 M_a &= 101.1 \text{ lb-in} & n &= 2.5, S_{ut} = 64 \text{ ksi}, S_y = 54 \text{ ksi}, K_A = 0.896 \\
 M_m &= 54.54 \text{ lb-in} & K_f &= 1.98, K_{fs} = 2.126, K_C = K_D = K_E = 1 \\
 (T_2)_a &= 380 \text{ lb-in} & S_e &= K_A K_B K_C K_D K_E S'_e & S'_e = 0.5 S_{ut} = 32 \text{ ksi} \\
 (T_2)_m &= 205 \text{ lb-in} & S_e &= K_B (0.896)(32) \text{ ksi} \rightarrow K_B = ?
 \end{aligned}$$

DE - Goodman equation

$$d = \left(\frac{16n}{\pi} \left\{ \frac{1}{S_e} [4(K_f M_a)^2 + 3(K_{fs} T_a)^2]^{1/2} + \frac{1}{S_{ut}} [4(K_f M_m)^2 + 3(K_{fs} T_m)^2]^{1/2} \right\} \right)^{1/3}$$

* 1st iteration: assume $d = 1 \text{ in.}$, $K_B = 0.879(1)^{-0.107} = 0.879$
 $S_e = (.879)(.896)(32) = 25.2 \text{ ksi} \rightarrow d = 0.962 \text{ in.}$

* 2nd iteration: assume $d = 0.962 \text{ in.}$, $K_B = 0.879(.962)^{-0.107} = 0.8826$
 $S_e = (.896)(.8826)(32) = 25.3 \text{ ksi} \rightarrow d = 0.961 \text{ in.}$

DE - gerber equation: $d = \left(\frac{8nA}{\pi S_e} \left\{ 1 + \left[1 + \left(\frac{2BS_e}{AS_{ut}} \right)^2 \right]^{1/2} \right\} \right)^{1/3}$ $A = \sqrt{4(K_f M_a)^2 + 3(K_{fs} T_a)^2}$
 $B = \sqrt{4(K_f M_m)^2 + 3(K_{fs} T_m)^2}$

$$\begin{aligned}
 A &= (4(1.98 * 101.1)^2 + 3(2.126 * 380)^2)^{1/2} = 1,455.4 \text{ psi} \\
 B &= (4(1.98 * 54.54)^2 + 3(2.126 * 205)^2)^{1/2} = 785.17 \text{ psi}
 \end{aligned}$$

* 1st iteration, assume $d = 1 \text{ in.}$, $K_B = 0.879(1)^{-0.107} = 0.879$
 $S_e = (.896)(.879)(32) = 25.2 \text{ ksi} \rightarrow d = 0.915 \text{ in.}$

* 2nd iteration, assume $d = 0.915 \text{ in.}$, $K_B = 0.879(.915)^{-0.107} = 0.887$
 $S_e = (.896)(.887)(32) = 25.442 \text{ ksi} \rightarrow d = 0.912 \text{ in.}$

DE - ASME Elliptic : $d = \left\{ \frac{16n}{\pi} \left[4 \left(\frac{K_f M_a}{S_e} \right)^2 + 3 \left(\frac{K_{fs} T_a}{S_e} \right)^2 + 4 \left(\frac{K_f M_m}{S_y} \right)^2 + 3 \left(\frac{K_{fs} T_m}{S_y} \right)^2 \right]^{1/2} \right\}^{1/3}$

* 1st iteration, assume $d = 1 \text{ in.}$, $K_B = 0.879(1)^{-0.107} = 0.879$
 $S_e = (.896)(.879)(32) = 25.2 \text{ ksi} \rightarrow d = 0.912 \text{ in.}$

* 2nd iteration, assume $d = 0.912 \text{ in.}$, $K_B = 0.879(.912)^{-0.107} = 0.8877$
 $S_e = (.896)(.8877)(32) = 25.45 \text{ ksi} \rightarrow d = 0.909 \text{ in.}$

DE-Soderberg equation:

$$d = \left(\frac{16n}{\pi} \left\{ \frac{1}{S_e} [4(K_f M_a)^2 + 3(K_{fs} T_a)^2]^{1/2} + \frac{1}{S_y} [4(K_f M_m)^2 + 3(K_{fs} T_m)^2]^{1/2} \right\} \right)^{1/3}$$

* 1st iteration, assume $d = 1 \text{ in.}$, $k_B = 0.879(1)^{-0.107} = 0.879$

$$S_e = (.896)(.879)(32) = 25.2 \text{ ksi} \rightarrow d = 0.974 \text{ in.}$$

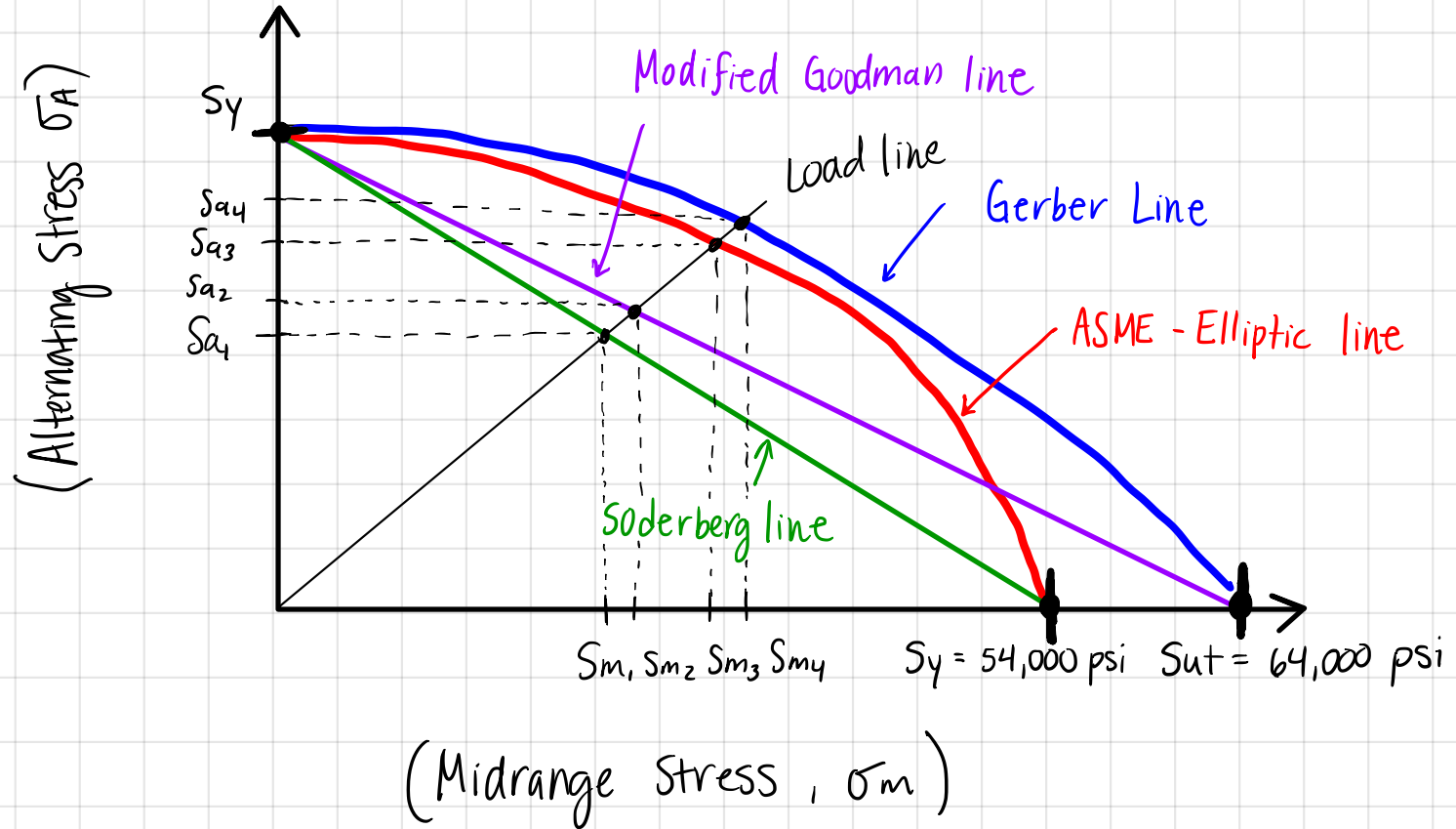
* 2nd iteration, assume $d = 0.974 \text{ in.}$, $k_B = 0.879(.974)^{-0.107} = 0.8815$

$$S_e = (.896)(.8815)(32) = 25.27 \text{ ksi} \rightarrow d = 0.973 \text{ in.}$$

Failure Criteria	Input Shaft Diameter (in.)	Output Shaft (in.)
Goodman	0.715	0.961
Gerber	0.677	0.912
ASME-Elliptic	0.675	0.909
Soderberg	0.723	0.973

From figure 6-27 in the book you can see that the Soderberg line is the most conservative meaning that the Soderberg equations will produce a larger diameter. Also from the figure you can see that Gerber and ASME Elliptic should yield really similar diameters for a certain portion of the graph.

Part B.) Fatigue diagram For shaft 1



* Diameters from Soderber criteria in part A.

$$D_i = 0.723 \text{ in. } D_o = 0.973 \text{ in.}$$

$$\sigma_a = \frac{32(101.1)}{\pi D_i^3} = \frac{1029.8}{D_i^3} \quad T_{a,1} = \frac{16(126.667)}{\pi D_i^3} = \frac{645.1}{D_i^3}$$

$$\sigma_m = \frac{32(54.54)}{\pi D_i^3} = \frac{555.54}{D_i^3} \quad T_{m,1} = \frac{16(68.333)}{\pi D_i^3} = \frac{348.02}{D_i^3}$$

For input:

$$\bar{\sigma}_{a,1} = \frac{1029.8}{(0.723)^3} = 2,724.8 \text{ psi} \quad \bar{T}_{a,1} = \frac{645.1}{(0.723)^3} = 1,706.9 \text{ psi}$$

$$\bar{\sigma}_{m,1} = \frac{555.54}{(0.723)^3} = 1,469.9 \text{ psi} \quad \bar{T}_{m,1} = \frac{348.02}{(0.723)^3} = 656.25 \text{ psi}$$

For output:

$$\bar{\sigma}_{a,2} = \frac{1029.8}{(0.973)^3} = 1,117.9 \text{ psi} \quad \bar{T}_{a,2} = \frac{1,935.3}{(0.973)^3} = 2,100.9 \text{ psi}$$

$$\bar{\sigma}_{m,2} = \frac{555.54}{(0.973)^3} = 603.1 \text{ psi} \quad \bar{T}_{m,2} = \frac{1,044.1}{(0.973)^3} = 1,133.4 \text{ psi}$$

$$\sigma_a' = \left\{ \left[K_f \sigma_{a, \text{Bend}} + \frac{K_f \sigma_{a, \text{Axial}}}{0.85} \right]^2 + 3 \left[k_{fs} (T_a) \right]^2 \right\}^{1/2}$$

$$S_a = n \sigma_a'$$

$$\sigma_m' = \left\{ \left[K_{fm} (\sigma_m)_{\text{Bend}} + K_f (\sigma_m)_{\text{Axial}} \right]^2 + 3 [k_{fs} s_m T_m]^2 \right\}^{1/2}$$

$$S_m = n \sigma_m'$$

For shaft 1:

$$\sigma_a' = 8,283.31$$

$$\sigma_m' = 3782.87$$

$$\text{DE - Goodman: } \frac{\sigma_a}{S_e} + \frac{\sigma_m}{S_{ut}} = \frac{1}{n} \quad S_e = (.896)(.910)(32) = 26.09 \text{ ksi}, S_{ut} = 64 \text{ ksi}$$

$$K_B = (.879)(.723)^{-10^7} = .910$$

$$\frac{8.283}{26.09} + \frac{3.782}{64} = \frac{1}{n} \Rightarrow n = 2.655 \quad \underline{S_a = 21,996 \quad S_m = 10,043}$$

$$\text{Soderberg: } \frac{\sigma_a}{S_e} + \frac{\sigma_m}{S_y} = \frac{1}{n} \quad \text{from part A: } S_e = 26.1 \text{ ksi}, S_y = 54 \text{ ksi}$$

$$\frac{8.283}{26.1} + \frac{3.782}{54} = \frac{1}{n} \Rightarrow n = 2.581 \quad \underline{S_a = 21,382 \quad S_m = 9,765}$$

$$\text{DE Gerber: } \frac{1}{n} = \frac{8A}{\pi d^3 S_e} \left\{ 1 + \left[1 + \left(\frac{2BS_e}{AS_{ut}} \right)^2 \right]^{1/2} \right\} \quad A = \sqrt{4(K_f M_a)^2 + 3(K_{fs} T_a)^2}$$

$$B = \sqrt{4(K_f M_m)^2 + 3(K_{fs} T_m)^2}$$

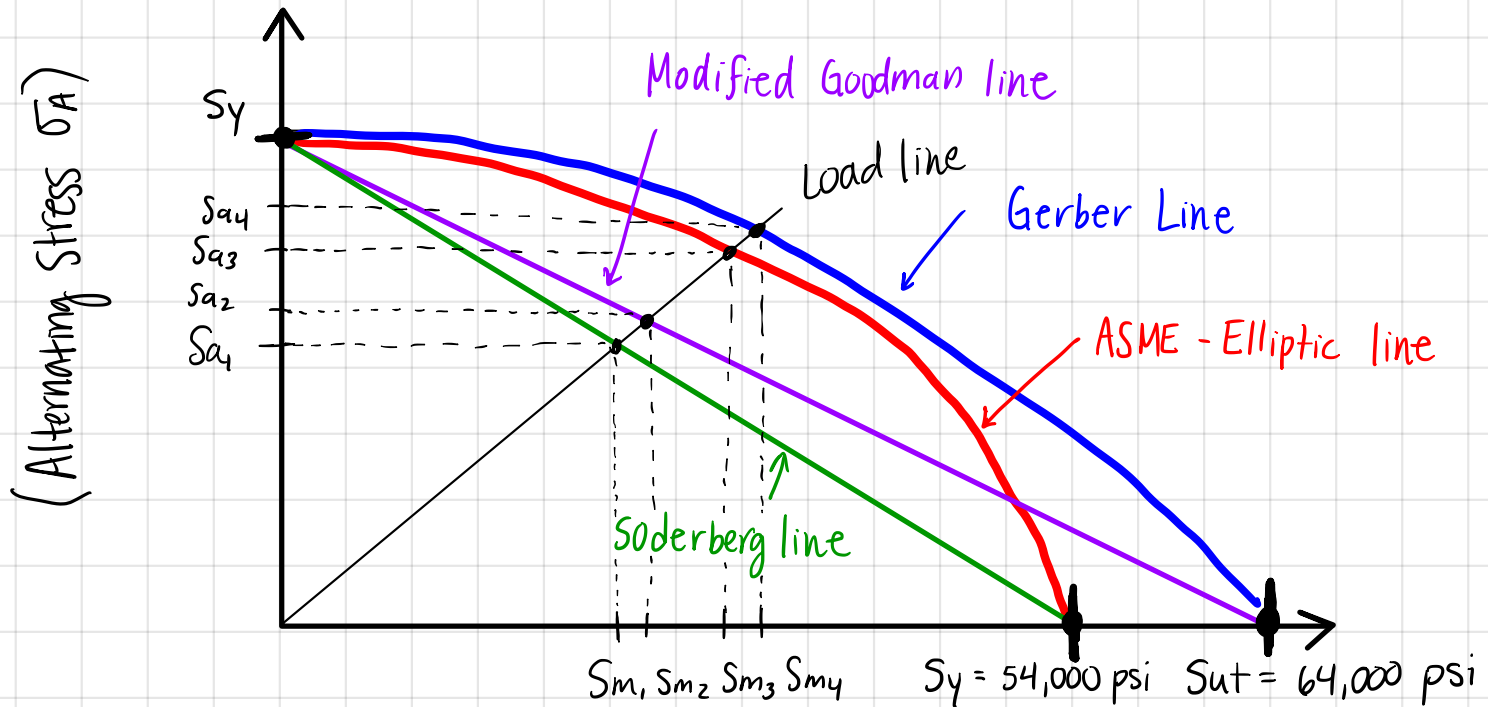
$$A = 614.69 \quad S_e = 26.1 \text{ ksi} \quad n = 3.01 \Rightarrow S_a = 24,938.1 \text{ psi}$$

$$B = 331.61 \quad S_m = 11,388.87 \text{ psi}$$

$$\text{DE - ASME elliptic: } \frac{1}{n} = \frac{16}{\pi d^3} \left[4 \left(\frac{K_f M_a}{S_e} \right)^2 + 3 \left(\frac{K_{fs} T_a}{S_e} \right)^2 + 4 \left(\frac{K_f M_m}{S_y} \right)^2 + 3 \left(\frac{K_{fs} T_m}{S_y} \right)^2 \right]^{1/2}$$

$$n = 3.048 \quad \underline{S_a = 25,247.5 \text{ psi} \quad S_m = 11,530.2 \text{ psi}}$$

Fatigue diagram For shaft 2



(Midrange Stress , σ_m)

For shaft 1 : $D_o = 0.973 \text{ in.}$

$$\sigma_a = 8,046 \quad \sigma_m = 4,341.04$$

$$\text{DE - Goodman : } \frac{\sigma_a}{S_e} + \frac{\sigma_m}{S_{ut}} = \frac{1}{n} \quad S_e = (.896)(.910)(32) = 26.09 \text{ ksi}, S_{ut} = 64 \text{ ksi}$$

$$K_B = (.879)(.723)^{-107} = .910$$

$$\frac{8.046}{26.09} + \frac{4.314}{64} = \frac{1}{n} \Rightarrow n = 2.662 \quad S_a_2 = 21,417 \quad S_m_2 = 11,555$$

$$\text{Soderberg : } \frac{\sigma_a}{S_e} + \frac{\sigma_m}{S_y} = \frac{1}{n} \quad \text{from part A : } S_e = 26.1 \text{ ksi}, S_y = 54 \text{ ksi}$$

$$\frac{8.046}{26.1} + \frac{4.314}{54} = \frac{1}{n} \rightarrow n = 2.567 \quad S_a_1 = 20,728 \quad S_m_1 = 11,184.5 \text{ psi}$$

$$\text{DE Gerber : } \frac{1}{n} = \frac{8A}{\pi d^3 S_e} \left\{ 1 + \left[1 + \left(\frac{2BS_e}{AS_{ut}} \right)^2 \right]^{1/2} \right\} \quad A = \sqrt{4(K_f M_a)^2 + 3(K_{fs} T_a)^2}$$

$$B = \sqrt{4(K_f M_m)^2 + 3(K_{fs} T_m)^2}$$

$$A = 1,455.4 \text{ psi} \quad S_e = 26.1 \text{ ksi} \quad n = 3.099 \Rightarrow S_a_4 = 24,936.5 \text{ psi}$$

$$B = 785.17 \text{ psi} \quad S_m_4 = 13,453.95 \text{ psi}$$

$$\text{DE - ASME elliptic : } \frac{1}{n} = \frac{16}{\pi d^3} \left[4 \left(\frac{K_f M_a}{S_e} \right)^2 + 3 \left(\frac{K_{fs} T_a}{S_e} \right)^2 + 4 \left(\frac{K_f M_m}{S_y} \right)^2 + 3 \left(\frac{K_{fs} T_m}{S_y} \right)^2 \right]^{1/2}$$

$$n = 3.13 \quad S_a_3 = 25,245 \text{ psi} \quad S_m_3 = 13,620.4 \text{ psi}$$

Design of a 40kW Biomass Pellet Burner

MAE 436/536 Fall 2019

Team 3

Nick Vincetic, Anirudh Lakshmi Narasimha Prasad, Matilda Koa,
Armando Chavez

1. PROBLEM STATEMENT

Biomass pellet burners are one of the cheapest alternative fuel energy systems that can potentially have a wide variety of applications. They can be specifically useful for the farming industry where large amounts of biomass are produced, commercial and residential sectors as a replacement to traditional fossil fuel burners. Currently, 3kW burner is available to meet smaller energy demands but a strong need for a 40kW burner is expressed by a large market share and our project seeks to address this. Also, currently available pellet burners are exclusive to the European market and are not readily available in the United States. Emissions are a major factor plaguing most burners with stricter emission norms being implemented year after year. The choice of fuel plays a major role in the performance as well as in the emissions from the pellet burner. Overall, the task before us is to design a pellet burner that is cost-effective, limits emission without compromising efficiency and is compact and portable.

2. VALUE PROPOSITION

Keeping all the above factors in mind, during our initial research we found literature that had performed experiments to optimize efficiency while minimizing emissions. This was the driving force for our design where we have a system that has very little emission, well below the current environmental standards without sacrificing a huge chunk of efficiency. The emissions are highly dependent on the fuel composition and based on the literature we found that sesame seed stalk is a fuel that is easily available widely in the US, especially in the South and South Western regions where sesame is grown as a commercial crop.

This fuel along with providing the benefit of being widely available at a lower cost also had a similar composition to the pellets used in the literature that optimized efficiency and emissions. Thus we could estimate that our system will produce about 76g/GJ of NOx when burning with 39% excess air with an efficiency of 75% that is way below the current European norms of 150g/GJ. This is advantageous to our system as there is no need for expensive catalytic converters, fuel gas recirculation system which helps in reducing cost significantly.

Our system also has a very innovative ash removal system in the form of a rotating combustion chamber with holes along with a modular ash compactor, which makes it very easy to remove and repurpose ash in any way the customer sees fit. The ash compactor is made similar to a trash can on wheels which can hold large volumes of ash while being easy to remove and clean. This helps keep maintenance costs down by having to dispose of the ash only once per week or so.

We estimate that with high volume manufacturing and some government subsidy for the use of an alternative fuel system we can get the cost down to below \$1000. At this price point, we get a big market advantage compared to other expensive alternatives and added to this the fact that being a US based company gives us a very large target audience.

A study conducted through the United States patent office showed that there are a few currently issued patents similar to the design proposed. In table 1 below, shows the four patents that have the closest similarity to our design. Each one of the patents claims a slightly different pellet burning system for use in various applications. It is the assumption then of the team, that we do have intellectual property that can be patented should we decide to go down that road. From the patent search of more than two dozen wood pellet

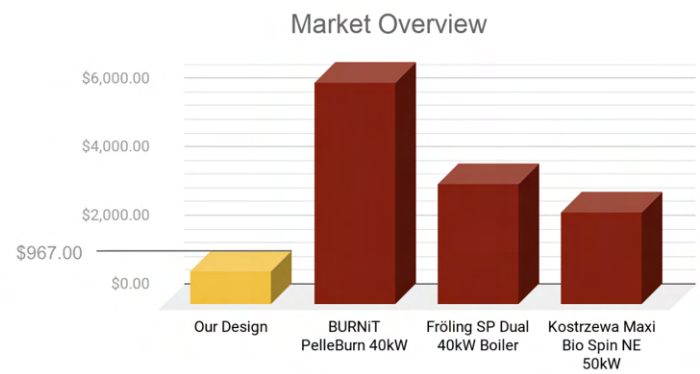


Fig 1: Market Overview

burning systems, many are similar but have slight differences that allow for enough variability for a unique patent, and our team believes our design qualifies for that category as well.

Patent NO.	Description on Similarity to Proposed Design
5,137,012	This invention claims a firebox defining a combustion chamber with a pellet burner in the firebox, with a feed surface adjacent to combustion zone. An ash pan for receiving the ashes of the pellet burner and means for supplying secondary air to a secondary combustion cavity.
5,873,356	This invention claims a stove housing having a top, bottom, and side panels with a fire box access door. A burn pot for burning wood pellets therin and disposed on said fire box floor and centered upon. A heat exchanger with panels attached to fire box walls in a spaced relationship to form a combustion air and exhaust gas channel.
7,861,707	This invention claims a gravity feed natural draft pellet stove with a feed tube extending upwardly from the top side of the vent tube. A primary combustion area comprising of a burn unit and a pellet receptacle. A secondary combustion area comprising of a burn box disposed below the lower vent feed opening. The chamber is configured to receive pellet fuel from primary burn chamber and multiple openings for receiving air into the secondary combustion area.
10,077,904	A wood pellet burner assembly comprising of a main support enclosure for the assembly, an enclosed air chamber fed with combustion air from a burner fan and having combustion gas outlet into the wood pellet boiler. A fixed fuel supporting apertured gate mounted above a base wall forming part of the main support enclosure. Finally, a scraper sub assembly for traversing the fixed fuel supporting apertured gate for delivery of residual ash on the fixed fuel grate.

Table 1: Patent Search Results (Four Closest in Similarity)

3. TECHNICAL MERIT

The overview of the design proposed in this report is listed in fig 1 below. The prototype features an air blower that delivers air at **298K** at a rate of **1.73m³/min** to the combustion chamber. The pellet feeder system rotates at **0.15 rpm** to deliver pellets at a rate of **10.8 kg/hr**. The rotating combustion chamber rotates at an rpm of 1 to dislodge ash products from the combustion chamber to prevent build up and manual cleaning. This ash collector is then sized to be emptied only once per week to allow for very minimal maintenance of the system. Finally, the heat exchanger is a versatile hookup to a variety of systems that the customer might need. This will allow for the most flexibility with the product and enable a wide range of applications to use the heat energy. The fuel Sesame seed stalk is modelled as shown in the table below to perform the technical calculations along with some other important combustion characteristics. Detailed calculations can be seen in Appendix 1.

A diagram has been generated in fig 3 below that depicts the potential hookup and installation of our system into an existing building. The

Fuel	Sesame stalk modelled as C ₁ H _{1.4} O _{0.6}
Lower Heating value	17.79 MJ/kg
Air/Fuel Ratio	11.23 kg of air/kg of fuel
Equivalence Ratio	0.72
Adiabatic Flame Temperature	1510K
Burning rate	2.1*10 ⁻⁸ kg/s
Minimum Ignition Energy	0.55J

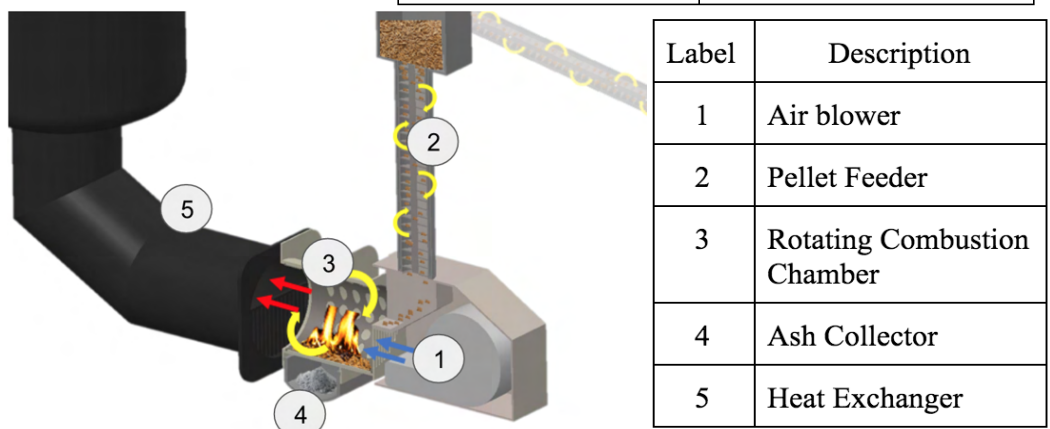


Fig 2: Design Schematic

general placement of water temperature sensors is listed so that the user is constantly aware of the performance of the pellet burner and can adjust the heat depending on their needs. Hookup of expansion vessels to reduce the amount of pressure going into the pellet burner's heat exchanger is listed as well because a big need to prevent buildup in water pressure which can potentially cause leaking issues.

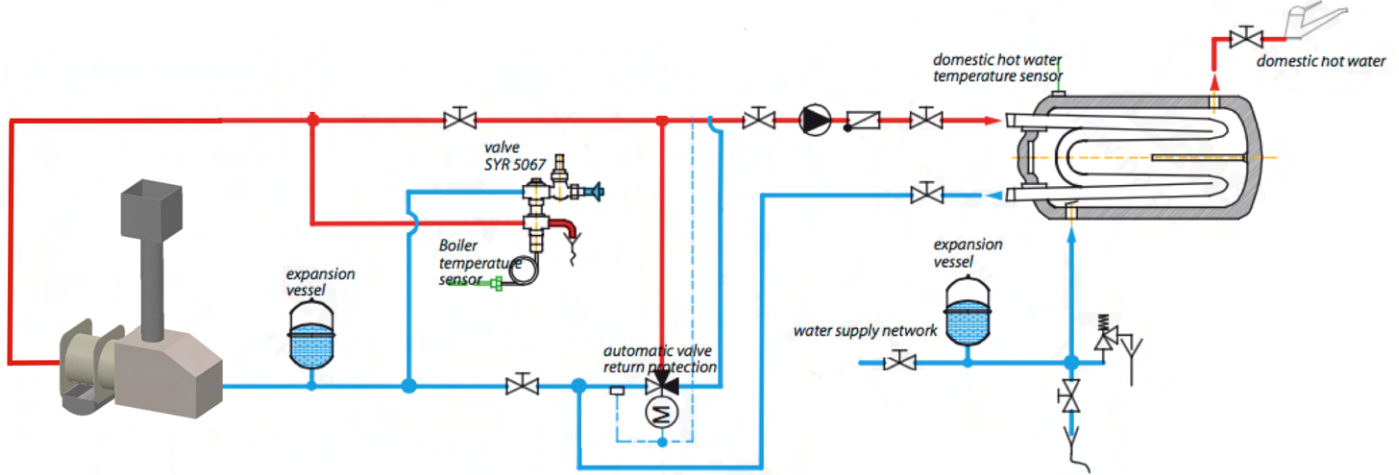


Fig 3: High Level Schematic of Installation for the Pellet Burning System

4. CONCLUSION AND FUTURE SCOPE

At the end of this phase of the project, we have a technically sound product design with a roadmap to refine and better it. We are in a good position where once we receive funding from a group of investors a prototype can be built and tested according to the timeline shown. Experiments need to be conducted in order to verify the emissions claim along with EPA certification needs to be obtained. Methods to improve efficiency without changing emissions will be another area of focus. Getting costs down to ~\$1000 per unit is going to be the major focus of future studies.

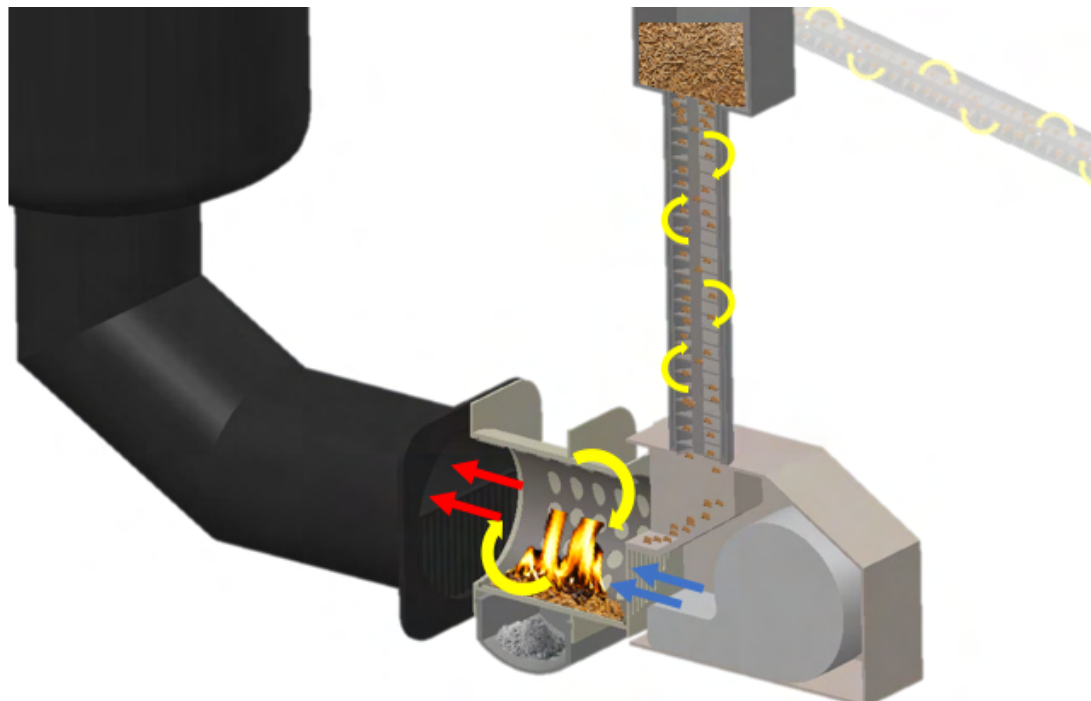


Fig 4: Company Roadmap Through Q3 2021

APPENDIX

PROJECT CALCULATIONS

CONTENTS			
KEY FEATURES	Pg. 5	EXPECTED EMISSIONS AND HOW TO PREDICT THEM	Pg. 12
FUEL SELECTION	Pg. 5	ESTIMATING THE EFFICIENCY	Pg. 13
MODELING OF FUEL AS $C_xH_yO_z$	Pg. 6	CALCULATING THE MASS FLOW RATE OF FUEL AND AIR	Pg. 13
NASA CEA ANALYSIS FOR STOICHIOMETRIC CONDITIONS	Pg. 7	SIZING THE BLOWER	Pg. 14
DETERMINING EQUIVALENCE RATIO	Pg. 9	DETERMINING THE BURNING RATE	Pg. 14
DETERMINING THE EQUIVALENCE RATIO FOR OUR SYSTEM	Pg. 10	DETERMINING THE MINIMUM IGNITION ENERGY	Pg. 16
NASA CEA ANALYSIS FOR FUEL LEAN CONDITIONS	Pg. 10	EXTRA CAD FILES AND IMAGES	Pg. 16



Schematic of Pellet Burner Design

KEY FEATURES

- Blower: Delivers **0.034 kg/s** of air at **298K** to the combustion chamber, or **1.73 m³/min.**
- Pellet delivery system: Rotates at **0.15 rpm** to deliver pellets at a rate of **0.003 kg/s** to the combustion chamber.
- Combustion chamber has an inner housing rotating at **1 rpm** to dislodge ash by products and force them into the collection chamber below.
- Ash removal system: sized so that the user has to empty the ash **1** time per week (very low maintenance).
- General hookup for application in a wide variety of systems needing heat exchangers.

1. FUEL SELECTION

Fuel assumed: **Sesame Stalk**

FUEL COMPOSITION

C	48.62% wt
H	05.65% wt
O	37.89% wt
N	00.57% wt
ASH	07.26% wt
MOISTURE	09.53% wt

Source: Daniel Neves, Henrik Thunman, Arlindo Matos, Luís Tarelho, Alberto Gómez-Barea, Characterization and prediction of biomass pyrolysis products, Progress in Energy and Combustion Science 37 (2011) 611 - 630

MASS FRACTION

Y_C	0.4440
Y_H	0.0515
Y_O	0.3460
Y_N	0.0052
Y_{ash}	0.0660
$Y_{moisture}$	0.0870

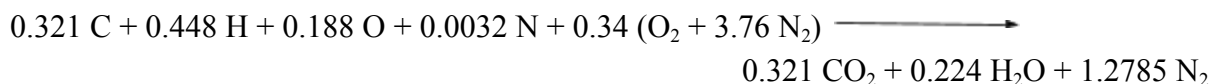
$$MW_{\text{mixture}} = \frac{1}{\sum \frac{Y}{MW}} = \frac{1}{\frac{0.444}{12} + \frac{0.0515}{1} + \frac{0.346}{16} + \frac{0.0052}{14} + \frac{0.087}{18}} = 8.699$$

MOLE FRACTION

X _C	0.3210
X _H	0.4480
X _O	0.1880
X _N	0.0032
X _{moisture}	0.0420

2. MODELING OF FUEL AS C_xH_yO_z

Ignoring moisture and ash, since HHV available in source is for dry fuel



Ignoring N as it is present in very small quantities fuel is modeled as C_xH_yO_z

where x=0.321, y=0.448, z=0.188

This can be simply written as C₁H_{1.4}O_{0.6}

The balanced reaction now becomes:



This was initially approximated as C₂H₂O but the values obtained for HHV was very far from the one available in literature.

So, remodeled as CH₂O or HCHO (formaldehyde)

HIGHER HEATING VALUE

Heat of Combustion = 570.7 KJ/mol

Source:<https://pubchem.ncbi.nlm.nih.gov/source/hsdb/164#section=Heat-of-Combustion&fullscreen=true>

Converting to mass basis gives heat of combustion (HHV) =
 $570.7 \frac{KJ}{mol} * \frac{1}{30*10^{-3}} \frac{mol}{kg} = 19.023 \frac{MJ}{kg}$

This value is very close to the higher heating value of $19.10 \frac{MJ}{kg \text{ of dry fuel}}$

STOICHIOMETRIC AIR FUEL RATIO

Stoichiometric Air fuel ratio for dry fuel excluding moisture and ash is calculated as

$$\frac{A}{F} = \frac{m_{air}}{m_{fuel}} = \frac{n_{air} * MW_{air}}{n_{fuel} * MW_{fuel}} = \frac{1.35 * 4.76 * 28.87}{1 * 23} = 8.06 \frac{kg \text{ of air}}{kg \text{ of fuel}}$$

Thus, HCHO was used in NASA CEA to calculate an approximate adiabatic flame temperature and product species concentration.

3. NASA CEA ANALYSIS FOR STOICHIOMETRIC CONDITIONS

```
*****
NASA-GLENN CHEMICAL EQUILIBRIUM PROGRAM CEA2, FEBRUARY 5, 2004
BY BONNIE MCBRIDE AND SANFORD GORDON
REFS: NASA RP-1311, PART I, 1994 AND NASA RP-1311, PART II, 1996
*****
### CEA analysis performed on Fri 22-Nov-2019 23:38:19
# Problem Type: "Assigned Enthalpy and Pressure"
prob case=_____2820 hp
# Pressure (1 value):
p,atm= 1
# Oxidizer/Fuel Wt. ratio (1 value):
o/f= 8.06
# You selected the following fuels and oxidizers:
reac
fuel HCHO,formaldehyde wt% =100.0000 t,k= 298.000
```

```

oxid Air      wt% = 100.0000 t,k= 298.000

# You selected these options for output:
# short version of output
output short
# Proportions of any products will be expressed as Mass Fractions.
output massf
# Heat will be expressed as si units
output siunits

# Input prepared by this script:prepareInputFile.cgi

### IMPORTANT: The following line is the end of your CEA input file!
end

```

THERMODYNAMIC EQUILIBRIUM COMBUSTION PROPERTIES AT ASSIGNED
PRESSURES

CASE = _____

REACTANT	WT FRACTION	ENERGY	TEMP
	(SEE NOTE)	KJ/KG-MOL	K
FUEL HCHO,formaldehyde	1.0000000	-108585.308	298.000
OXIDANT Air	1.0000000	-129.895	298.000

O/F= 8.06000 %FUEL= 11.037528 R,EQ.RATIO= 0.666998 PHI,EQ.RATIO= 0.571359

THERMODYNAMIC PROPERTIES

P, BAR	1.0132
T, K	1851.51
RHO, KG/CU M	1.9133-1
H, KJ/KG	-403.15
U, KJ/KG	-932.73
G, KJ/KG	-17314.3
S, KJ/(KG)(K)	9.1337

M, (1/n)	29.069
(dLV/dLP)t	-1.00011
(dLV/dLT)p	1.0042
Cp, KJ/(KG)(K)	1.4465
GAMMAS	1.2489
SON VEL,M/SEC	813.3

MASS FRACTIONS

*Ar	0.01149
*CO	0.00013
*CO2	0.16201
H2O	0.06594
*NO	0.00292
NO2	0.00001
*N2	0.67046
*O	0.00003
*OH	0.00050
*O2	0.08651

* THERMODYNAMIC PROPERTIES FITTED TO 20000.K

NOTE. WEIGHT FRACTION OF FUEL IN TOTAL FUELS AND OF OXIDANT IN TOTAL OXIDANTS

Clearly, 1851K is a high temperature that cannot be sustained by the combustion chamber materials.

Also burning at stoichiometric amounts leads to emissions much larger than if we burn fuel lean.

4. DETERMINING EQUIVALENCE RATIO

To determine an optimum operating air fuel ratio, we turn to a paper on optimizing efficiency and emissions by the University of Leeds in the United Kingdom, that performed an analysis for a 350kW biomass pellet burner. They used 5 different pellets (namely A, B, C, D, E) to study the optimum efficiency of operation at which there is minimum CO emission along with acceptable NOx emissions by the EU pollution control board.

Pellet E used in this study is very similar in composition and properties to the fuel we have used here and hence some characteristics from their analysis were used in our calculation.

Source: Mohamed A. Altaher, Gordon E. Andrews, Bernard M. Gibbs, Seyed A. Hadavi, Hu Li, Emma Jones and Mark Mercer, PARTICULATE EMISSIONS FROM A 350 kW WOOD PELLET HEATER, First International Biomass Emissions Conference – Leeds University Sept. 14-15, 2015.

The composition of pellet E in the above source is defined having a Chemical formula on the basis of $C_xH_yO_zN_w$ on a fly ash free basis (daf) as $C_1H_{1.58}O_{0.66}N_{0.09}$ which is very close to $C_1H_{1.4}O_{0.6}$ used for this calculation.

This source recommends the use of 39% excess air in order to minimize CO and NO_x emissions while maintaining an optimal thermal efficiency.

39% excess air indicates a new air mole fraction of 1.39 times existing air mole fraction. So new air mole fraction = 1.39*1.35 = 1.88

5. DETERMINING THE EQUIVALENCE RATIO FOR OUR SYSTEM

The balanced chemical equation now is:



Calculating the air fuel ratio again

$$\frac{A}{F} = \frac{m_{air}}{m_{fuel}} = \frac{n_{air} * MW_{air}}{n_{fuel} * MW_{fuel}} = \frac{1.88 * 4.76 * 28.87}{1 * 23} = 11.23 \frac{\text{kg of air}}{\text{kg of fuel}}$$

Equivalence ratio = (A/F)_s / (A/F)_{actual} = 8.06/11.23 = 0.72

6. NASA CEA ANALYSIS FOR FUEL LEAN CONDITIONS

Performing a CEA analysis at this equivalence ratio yields the following:

```
*****
NASA-GLENN CHEMICAL EQUILIBRIUM PROGRAM CEA2, FEBRUARY 5, 2004
BY BONNIE MCBRIDE AND SANFORD GORDON
REFS: NASA RP-1311, PART I, 1994 AND NASA RP-1311, PART II, 1996
*****
### CEA analysis performed on Sat 23-Nov-2019 00:05:14
# Problem Type: "Assigned Enthalpy and Pressure"
prob case=_____ 2820 hp
# Pressure (1 value):
p,atm= 1
```

```

# Oxidizer/Fuel Wt. ratio (1 value):
o/f= 11.23

# You selected the following fuels and oxidizers:
reactants
fuel HCHO,formaldehyde wt% = 100.0000 t,k= 298.000
oxid Air wt% = 100.0000 t,k= 298.000

# You selected these options for output:
# short version of output
output short
# Proportions of any products will be expressed as Mass Fractions.
output massf
# Heat will be expressed as si units
output siunits

# Input prepared by this script:prepareInputFile.cgi

### IMPORTANT: The following line is the end of your CEA input file!
end

```

THERMODYNAMIC EQUILIBRIUM COMBUSTION PROPERTIES AT ASSIGNED

PRESURES

CASE = _____

REACTANT	WT FRACTION	ENERGY	TEMP
	(SEE NOTE)	KJ/KG-MOL	K
FUEL HCHO,formaldehyde	1.0000000	-108585.308	298.000
OXIDANT Air	1.0000000	-129.895	298.000

O/F= 11.23000 %FUEL= 8.176615 R,EQ.RATIO= 0.511070 PHI,EQ.RATIO= 0.410076

THERMODYNAMIC PROPERTIES

P, BAR 1.0132

T, K 1510.66

RHO, KG/CU M 2.3433-1

H, KJ/KG -299.82

U, KJ/KG -732.21

G, KJ/KG -13607.2

S, KJ/(KG)(K) 8.8090

M, (1/n) 29.048

(dLV/dLP)t -1.00001

(dLV/dLT)p 1.0003

Cp, KJ/(KG)(K)	1.3194
GAMMAS	1.2772
SON VEL,M/SEC	743.1

MASS FRACTIONS

*Ar	0.01186
*CO2	0.12029
H2O	0.04903
*NO	0.00093
NO2	0.00001
*N2	0.69300
*OH	0.00004
*O2	0.12483

* THERMODYNAMIC PROPERTIES FITTED TO 20000.K

NOTE. WEIGHT FRACTION OF FUEL IN TOTAL FUELS AND OF OXIDANT IN TOTAL OXIDANTS

The CEA analysis shows that the adiabatic flame temperature would be around 1500K, which is better than the 1850K obtained previously. Even though this is a large number it only represents the upper bound for temperature as the actual reaction mechanism produce large number of products not shown in the analysis that can act as a heat sink. We have only considered the gas phase volatiles reaction and have ignored the role of ash in this reaction which would also act as a large heat sink. Moreover, since the walls are not insulated the adiabaticity of the burner is lost. All this leads to a much lower temperature than predicted by NASA CEA. Since the only way to truly estimate the temperature correctly is to measure it experimentally, this is the closest method we have to obtain at least a “worst case scenario” temperature value which absolutely should not be achieved or exceeded for optimal functioning of the pellet burner.

7. EXPECTED EMISSIONS AND HOW TO PREDICT THEM

Combustion of fuel results in the emission of NOx, SO2, CO, PM, and lead. In this project, the gas emissions we are expecting based on our fuel composition and NASA CEA analysis are CO and NOx (made up of NO and N02). When fuel was burned at stoichiometry with T-Adiabatic being 1851.51K, the concentration of the CO in terms of mass fraction was 0.00013, NO was 0.00292 and NO2 was 0.00001. When the combustion was performed in the fuel lean state, the results obtained from the NASA CEA analysis in terms of mass fraction were 0.00093 for NO and 0.00001 N02. CO was not produced at the fuel lean condition so we focused mainly on NOx emission. NO emissions concentration was greater than NO2 and this is explained in this paper titled “**Combustion and emission characteristics of a domestic boiler fired with**

pellets of pine, industrial wood wastes and peach stones”. It mentions that in small domestic boilers the temperature in the chamber is typically below 1300C therefore, NO formation via the fuel mechanism is expected to be the main source of NO_x emissions. Further explanation will be in the final report.

NO_x emission is considered one of the most dangerous emissions from a combustion system because it affects human health directly. Environmental Protection Agency(EPA) is trying to reduce its emissions based on the Clean Air ACT(CAA) by implementing policies such as the 1-hour NO₂ standard etc. They are also placing monitors in locations to help protect communities that are susceptible to NO_x related health issues. This shows the severity of NO_x emission and our work is limiting the emission of NO_x as much as possible. The NASA CEA analysis results above shows how it reduced drastically from 0.00292 to 0.00093.

8. ESTIMATING THE EFFICIENCY

From the above-mentioned source an average efficiency between 76.0 – 81.0% was obtained for various pellets for different air fuel ratios. Even though an efficiency is not clearly mentioned for pellet E which is closest to our fuel composition, based on the trends observed we can assume an efficiency between 75 and 80%. This is a very reasonable assumption as most biomass pellet burners currently commercially available have efficiencies with this range.

Using a very conservative approach to tackle this problem we assume the thermal efficiency achievable as 75%.

Thermal efficiency is defined as the ratio of power output by the pellet burner to the energy supplied by the fuel.

$$\eta_{th} = \frac{\text{Power output by the pellet burner}}{\text{Energy supplied by the fuel}} = \frac{\dot{W}}{m * \Delta h_c}$$

Where \dot{W} is the target power output i.e. 40kW and Δh_c is the lower heating value as the water will be in vapor state at the end of combustion.

9. CALCULATING MASS FLOW RATE OF FUEL AND AIR

LHV is just the higher heating value minus the enthalpy of vaporization

The latent heat for pellet E is mentioned in the literature specified above as 1.31 MJ/kg

So, LHV = HHV – LH = 19.10 – 1.31 = 17.79 MJ/kg of fuel

From all of these values \dot{m}_f can be calculated as $\dot{m}_f = \frac{\dot{W}}{\eta_{th} * \Delta h_c} = \frac{40 * 10^3}{0.75 * 17.79 * 10^6} = 0.003 \frac{kg}{s}$

This can be more appropriately expressed in terms of kg/hr.

So, $\dot{m}_f = 0.003 * 60 * 60 = 10.8 \text{ kg/hr}$

From the air fuel ratio mass flow rate of air can be calculated as

$$\frac{A}{F} = \frac{\dot{m}_{air}}{\dot{m}_{fuel}} = \frac{\dot{m}_{air}}{\dot{m}_{fuel}} \rightarrow \dot{m}_{air} = \dot{m}_{fuel} * \frac{A}{F} = 10.8 * 11.23 = 121.28 \frac{kg}{hr} \text{ or } 0.034 \text{ kg/s}$$

10. SIZING THE BLOWER

Once the mass flow rate of air is known we can size the blower as follows:

From the gas law we have $P * V = m * R * T$ which can also be written as

$$P * \dot{V} = \dot{m} * R * T \rightarrow \dot{V} = \frac{\dot{m} * R * T}{P}$$

Where P is the pressure = 1atm = 101325 Pa, R is the specific gas constant = $\frac{\bar{R}}{MW} = \frac{8314}{28.87} = 288 \frac{J}{kg-K}$ and T is the air inlet temperature = 298K (25C)

$$\dot{V} = \frac{\dot{m} * R * T}{P} = \frac{0.034 * 288 * 298}{101325} = 0.0288 \frac{m^3}{s} \text{ or } 1.73 \frac{m^3}{min}$$

A blower that can provide a volumetric flow rate of $1.73 \frac{m^3}{min}$ of air is required to operate the pellet burner at the desired conditions.

11. DETERMINING THE BURNING RATE

Typical pellets are 6 to 8mm in diameter and about 30 mm in length, this is cylindrical in shape and hence to simplify the analysis we assume a spherical pellet having the same volume as the cylindrical pellet

$$Volume\ of\ cylinder = \pi * r^2 * l = 3.1415 * 0.004 * 0.004 * 0.030 = 1.5 * 10^{-6} m^3$$

$$Volume\ of\ sphere = \frac{4}{3} * \pi * r^3 \rightarrow r = \left(\frac{3}{4\pi} * 1.5 * 10^{-6} \right)^{\frac{1}{3}} = 7.1\text{mm}$$

To determine the burning rate we now know the pellet diameter = 14.2 mm, $Y_{O_2,\infty} = 0.233$ at 1 atm. The particle temperature is assumed to be the same as the adiabatic flame temperature obtained from the CEA analysis above. Assuming a kinetic rate constant of 13.9 m/s as stated in the textbook burning rate can be calculated using either the one film or the two-film model.

Even though the two-film model is a more accurate model it is more tedious to work with and hence to simplify our analysis we use a one film model where the primary reaction is assumed to be $C + O_2 \longrightarrow CO_2$.

Circuit analogy is employed to find burning rate and diffusional resistance is first calculated using the formula $R_{diff} = \frac{v_1 + Y_{O_2,s}}{\rho D 4\pi r_s}$

To find density we use gas law as: $\rho = \frac{P}{\left(\frac{R_u}{MW_{mix}}\right)T_s} = \frac{101325}{\left(\frac{8314}{28}\right)*1510} = 0.226 \frac{kg}{m^3}$ where MW_{mix}

was calculated accounting for MW of gaseous fuel, air and products.

Mass diffusivity was estimated using a value for CO_2 in N_2 from appendix table D.1, corrected to 1510K via the relation that $D \propto T^{\frac{3}{2}}$.

$$D = \left(\frac{1510}{393} \right)^{1.5} * 1.6 * 10^{-5} = 1.2 * 10^{-4} m^2/s$$

Initially assuming $Y_{O_2,s} = 0$,

$$R_{diff} = \frac{v_1 + Y_{O_2,s}}{\rho D 4\pi r_s} = \frac{2.664+0}{0.226*1.2*10^{-4}*4*3.1415*0.0071} = 1.10 * 10^7 \frac{s}{kg}$$

The chemical kinetic resistance is calculated as:

$$R_{kin} = \frac{v_1 R_u T_s}{4\pi r_s^2 M W_{mix} k_c P} = \frac{2.66*8314*1510}{4*\pi*0.0071^2*28*13.9*101325} = 1366.76 \frac{s}{kg}$$

Since $R_{\text{diff}} \gg R_{\text{kin}}$ it is purely diffusion controlled but to justify our assumption about $Y_{O_2,s} = 0$ we will iterate if necessary, to obtain burning rate more accurately.

$$\dot{m}_c = \frac{Y_{O_2,\infty}}{R_{\text{diff}} + R_{\text{kin}}} = \frac{0.233}{1.10 \times 10^7 + 1366.76} = 2.1 \times 10^{-8} \frac{\text{kg}}{\text{s}}$$

From the circuit analogy

$$Y_{O_2,s} - 0 = \dot{m}_c * R_{\text{kin}} = 2.1 \times 10^{-8} * 1366.76 = 2.87 \times 10^{-5} = 0.0028\%$$

This value for $Y_{O_2,s}$ is very small and hence our assumption is justified. No further iterations are required.

12.DETERMINING MINIMUM IGNITION ENERGY

The minimum energy required to ignite the biomass pellet can be estimated from a simplified ignition analysis performed using a critical gas volume analogy

In order to maintain the surface of the biomass hot we need to choose the critical volume to be equal to the volume of the pellet. The pellet radius assuming a typical pellet dimensions and hence volume, is performed in the previous section. So, $R_{\text{critical}} = 7.1\text{mm}$

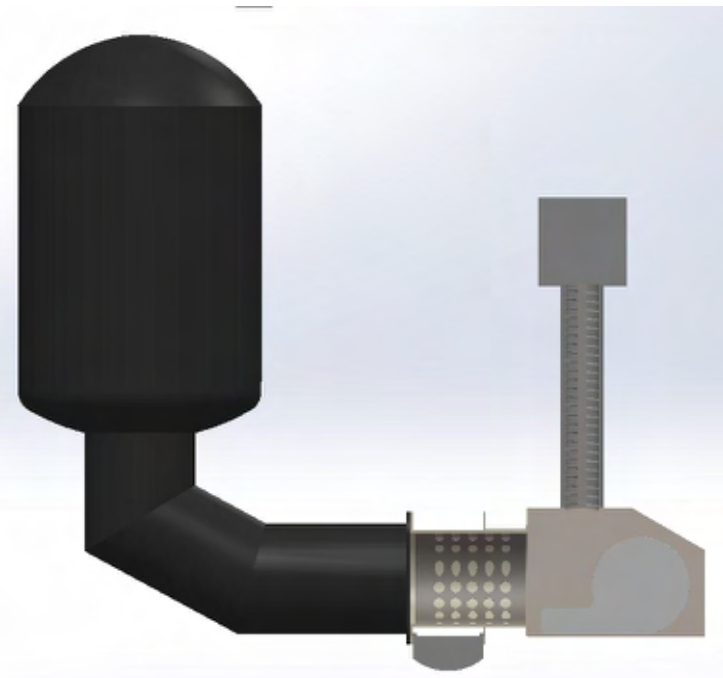
$$R_{\text{critical}} = \sqrt{6} * \frac{\alpha}{S_L} \rightarrow \frac{\alpha}{S_L} = \frac{R_{\text{critical}}}{\sqrt{6}} = \frac{0.0071}{\sqrt{6}} = 0.0029$$

Using this in the ignition energy formula given in Chapter 8

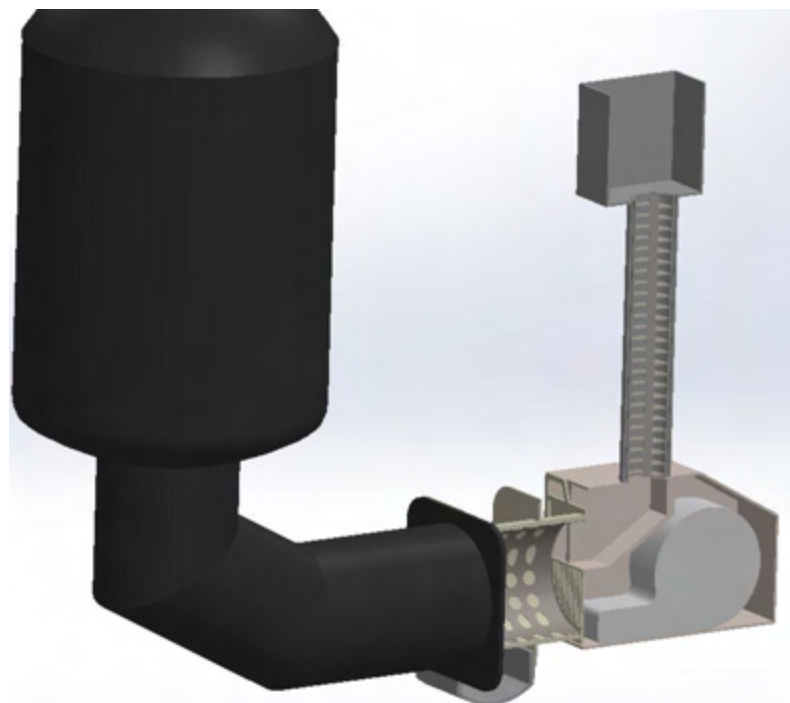
$$E_{\text{ignition}} = 61.6 * P * \left(\frac{Cp_u}{R_b} \right) * \left(\frac{T_b - T_u}{T_b} \right) * \left(\frac{\alpha}{S_L} \right)^3 = 61.6 * 101325 * \left(\frac{1292.32}{\frac{8314}{29}} \right) * \left(\frac{1510 - 298}{1510} \right) * (0.0029)^3 =$$

The minimum energy for ignition is 0.55J which is high since we are assuming a pellet which is typically of a much larger size than any other molecule that is considered for such analysis.

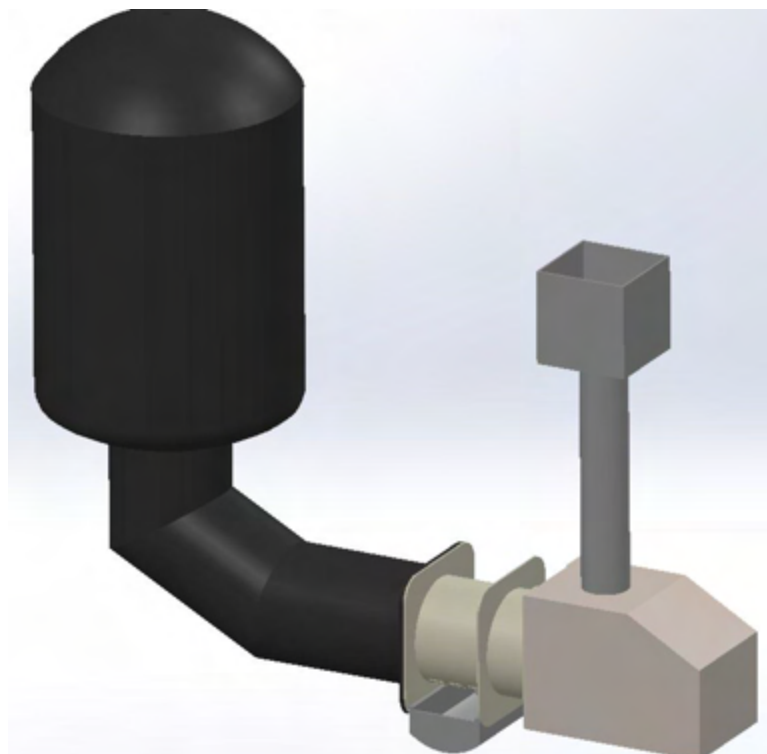
13.EXTRA CAD FILES/IMAGES



Side View Cross Section of Pellet Burner



Cross Section of Pellet Burner



Complete Burner Assembly